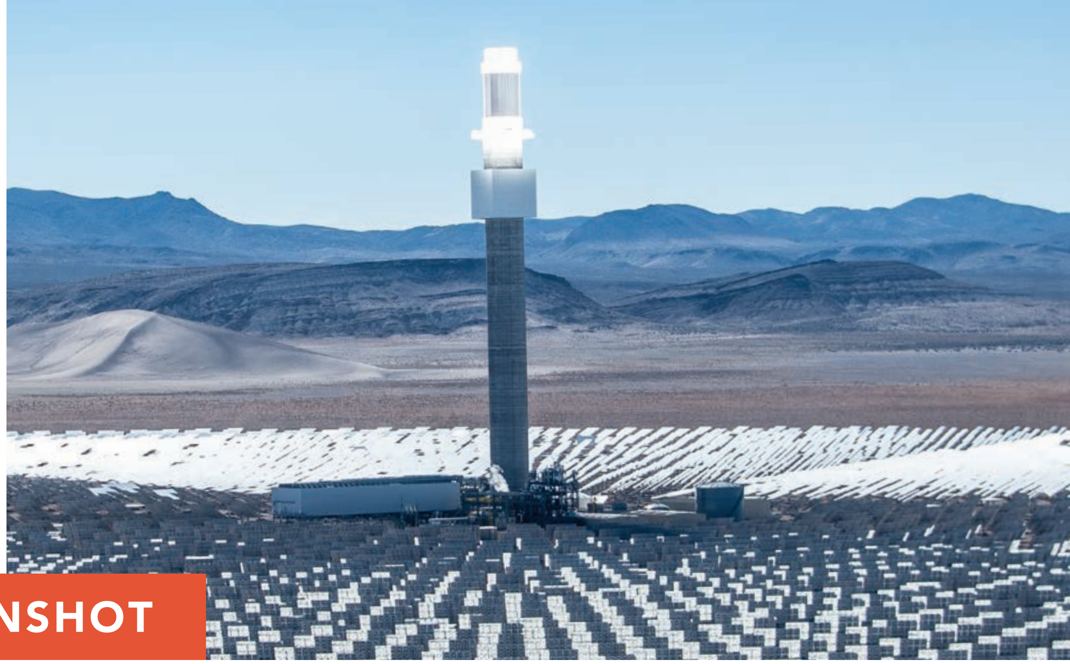

ON THE PATH TO SUNSHOT

# Advancing Concentrating Solar Power Technology, Performance, and Dispatchability

May 2016
NREL/TP-5500-65688
SAND2016-2237 R

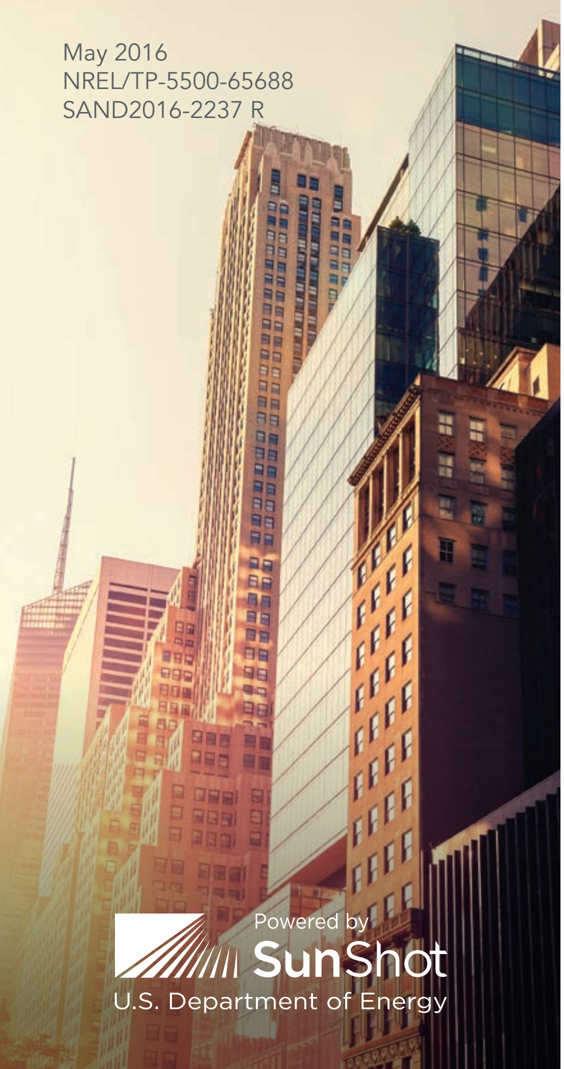

Powered by SunShot
U.S. Department of Energy

Sandia National Laboratories

NREL
NATIONAL RENEWABLE ENERGY LABORATORY

# On the Path to SunShot: Advancing Concentrating Solar Power Technology, Performance, and Dispatchability

Mark Mehos[1], Craig Turchi[1], Jennie Jorgenson[1],
Paul Denholm[1], Clifford Ho[2], and Kenneth Armijo[2]

[1] National Renewable Energy Laboratory
[2] Sandia National Laboratories

NREL is a national laboratory of the U.S. Department of Energy, Office of Energy Efficiency and Renewable Energy, operated by the Alliance for Sustainable Energy, LLC.

Sandia National Laboratories is a multi-program laboratory managed and operated by Sandia Corporation, a wholly owned subsidiary of Lockheed Martin Corporation, for the U.S. Department of Energy's National Nuclear Security Administration under contract DE-AC04-94AL85000.

Powered by SunShot
U.S. Department of Energy

Sandia National Laboratories

NREL
NATIONAL RENEWABLE ENERGY LABORATORY

SUGGESTED CITATION
Mehos, Mark, Craig Turchi, Jennie Jorgenson, Paul Denholm, Clifford Ho, and Kenneth Armijo. 2016. *On the Path to SunShot: Advancing Concentrating Solar Power Technology, Performance, and Dispatchability*. Golden, CO: National Renewable Energy Laboratory.
NREL/TP-5500-65688. http://www.nrel.gov/docs/fy16osti/65688.pdf.

*Cover photos (clockwise from top left): Solar Design Associates, Inc., NREL 08563; SolarReserve; Dennis Schroeder, NREL 30551; and iStock 000075760625*

## NOTICE

# Preface

The U.S. Department of Energy launched the SunShot Initiative in 2011 with the goal of making solar electricity cost-competitive with conventionally generated electricity by 2020. At the time this meant reducing photovoltaic and concentrating solar power prices by approximately 75%—relative to 2010 costs—across the residential, commercial, and utility-scale sectors. To examine the implications of this ambitious goal, the Department of Energy's Solar Energy Technologies Office (SETO) published the *SunShot Vision Study* in 2012. The study projected that achieving the SunShot price-reduction targets could result in solar meeting roughly 14% of U.S. electricity demand by 2030 and 27% by 2050—while reducing fossil fuel use, cutting emissions of greenhouse gases and other pollutants, creating solar-related jobs, and lowering consumer electricity bills.

The *SunShot Vision Study* (DOE 2012) also acknowledged, however, that realizing the solar price and deployment targets would face a number of challenges. Both evolutionary and revolutionary technological changes would be required to hit the cost targets, as well as the capacity to manufacture these improved technologies at scale in the U.S. Additionally, operating the U.S. transmission and distribution grids with increasing quantities of solar energy would require advances in grid-integration technologies and techniques. Serious consideration would also have to be given to solar siting, regulation, and water use. Finally, substantial new financial resources and strategies would need to be directed toward solar deployment of this magnitude in a relatively short period of time. Still the study suggested that the resources required to overcome these challenges were well within the capabilities of the public and private sectors. SunShot-level price reductions, the study concluded, could accelerate the evolution toward a cleaner, more cost-effective and more secure U.S. energy system.

That was the assessment in 2012. Today, at the halfway mark to the SunShot Initiative's 2020 target date, it is a good time to take stock: How much progress has been made? What have we learned? What barriers and opportunities must still be addressed to ensure that solar technologies achieve cost parity in 2020 and realize their full potential in the decades beyond?

To answer these questions, SETO launched the *On the Path to SunShot* series in early 2015 in collaboration with the National Renewable Energy Laboratory (NREL) and with contributions from Lawrence Berkeley National Laboratory (LBNL), Sandia National Laboratories (SNL), and Argonne National Laboratory (ANL). The series of technical reports focuses on the areas of grid integration, technology improvements, finance and policy evolution, and environment impacts and benefits. The resulting reports examine key topics that must be addressed to achieve the SunShot Initiative's price-reduction and deployment goals. The *On the Path to SunShot* series includes the following reports:

- Emerging Issues and Challenges with Integrating High Levels of Solar into the Electrical Generation and Transmission Systems (Denholm et al. 2016)
- Emerging Issues and Challenges with Integrating High Levels of Solar into the Distribution System (Palmintier et al. 2016)
- Emerging Opportunities and Challenges in Financing Solar (Feldman and Bolinger 2016)

- Utility Regulatory and Business Model Reforms for Addressing the Financial Impacts of Distributed Solar on Utilities (Barbose et al. 2016)
- The Role of Advancements in Photovoltaic Efficiency, Reliability, and Costs (Woodhouse et al. 2016)
- Advancing Concentrating Solar Power Technology, Performance, and Dispatchability (Mehos et al. 2016)
- Emerging Opportunities and Challenges in U.S. Solar Manufacturing (Chung et al. 2016)
- The Environmental and Public Health Benefits of Achieving High Penetrations of Solar Energy in the United States (Wiser et al. 2016).

Solar technology, solar markets, and the solar industry have changed dramatically over the past five years. Cumulative U.S. solar deployment has increased more than tenfold, while solar's levelized cost of energy (LCOE) has dropped by as much as 65%. New challenges and opportunities have emerged as solar has become much more affordable, and we have learned much as solar technologies have been deployed at increasing scale both in the U.S. and abroad. The reports included in this series, explore the remaining challenges to realizing widely available, cost-competitive solar in the United States. In conjunction with key stakeholders, SETO will use the results from the *On the Path to SunShot* series to aid the development of its solar price reduction and deployment strategies for the second half of the SunShot period and beyond.

# Acknowledgments

The authors thank the Solar Energy Technologies Office team for its support of this report and Robert Margolis of NREL for his management and oversight of the *On the Path to SunShot* report series. The following individuals provided valuable input during the analysis and publication process: Bradley Albert (Arizona Public Service), William Gould (SolarReserve), Barbara Goodman (NREL), Chuck Kutscher (NREL), David Mooney (NREL), Robin Newmark (NREL), Gian Porro (NREL), Hank Price (Abengoa), Joseph Stekli (DOE), and Mary Werner (NREL). The authors also thank Don Gwinner (NREL) and Mike Meshek (NREL) for their editorial assistance.

This work was funded by the Solar Energy Technologies Office of the U.S. Department of Energy (DOE) Office of Energy Efficiency and Renewable Energy (EERE) under Contract No. DE-AC36-08GO28308.

John Frenzl of NREL designed the covers for the *On the Path to SunShot* report series.

## List of Acronyms

| | |
|---|---|
| ARID | Advanced Research In Dry cooling |
| ARPA-E | Advanced Research Projects Agency-Energy |
| $C_C$ | capital cost |
| CC | combined cycle |
| CEC | California Energy Commission |
| CEPCI | Chemical Engineering Plant Cost Index |
| COG | California Cost of Generation model |
| COLLECTS | Concentrating Optics for Lower Levelized Energy CosTS |
| CPUC | California Public Utility Commission |
| CSP | concentrating solar power |
| CSP-TES | concentrating solar power with thermal energy storage |
| CT | combustion turbine |
| DNI | direct normal irradiance |
| DOE | U.S. Department of Energy |
| ELEMENTS | Efficiently Leveraging Equilibrium Mechanisms for Engineering New Thermochemical Storage |
| EPC | engineering, procurement, and construction |
| EPRI | Electric Power Research Institute |
| FCR | fixed charge rate |
| FIT | feed-in tariff |
| FOCUS | Full-Spectrum Optimized Conversion and Utilization of Sunlight |
| FOM | fixed operations and maintenance cost |
| HTF | heat-transfer fluid |
| IEA | International Energy Agency |
| IRENA | International Renewable Energy Agency |
| ISCCS | integrated solar combined-cycle system |
| ITC | investment tax credit |
| LBNL | Lawrence Berkeley National Laboratory |
| LCOE | levelized cost of electricity |
| LFR | linear Fresnel reflector |
| LPPA | levelized power purchase agreement |
| MENA | Middle East and North Africa |
| MSPT | molten-salt power tower |
| NG | natural gas |
| NREL | National Renewable Energy Laboratory |
| O&M | operations and maintenance |
| OTPSS | *On the Path to SunShot* |
| PCM | phase-change material |
| PV | photovoltaic(s) |
| REIPPP | Renewable Energy Independent Power Producer Procurement Program |
| RPS | renewable portfolio standard |
| SAM | System Advisor Model |
| SCA | solar collector assembly |
| $sCO_2$ | supercritical carbon dioxide |

| | |
|---|---|
| SEIA | Solar Energy Industries Association |
| SETO | Solar Energy Technologies Office |
| SM | solar multiple |
| SNL | Sandia National Laboratories |
| SolarMat | Solar Manufacturing Technology |
| SolarPACES | Concentrating Solar Power and Chemical Energy Systems |
| SVS | *SunShot Vision Study* |
| TES | thermal energy storage |
| VO&M | variable operations and maintenance |
| WACC | weighted average cost of capital |

# Executive Summary

Since the *SunShot Vision Study* (DOE 2012) was published, global deployment of concentrating solar power (CSP) has increased threefold to nearly 4,500 MW, with a similar threefold increase in operational capacity to 1,650 MW within the United States. Growth in U.S. CSP capacity has primarily been driven by policy support at the state and federal levels. State-driven renewable portfolio standards (RPSs), combined with a 30% federal investment tax credit (ITC) and federal loan guarantees, provided the opportunity for CSP developers to kick-start construction of CSP plants throughout the Southwest. Figure ES-1 demonstrates that deployment and private- and public-sector research and development have led to dramatic cost reductions that have placed CSP well on the path to reaching the U.S. Department of Energy's SunShot Initiative goal of 6 cents/kWh by 2020. In comparing the estimated capital costs from the *SunShot Vision Study* and the current analysis, we find that the predicted 2015 decline in tower costs was in line with expectations, primarily driven by reduced heliostat costs. Figure ES-1 shows the reduction in levelized cost of electricity (LCOE) for both parabolic trough and tower systems, in addition to the projected 2020 SunShot target.

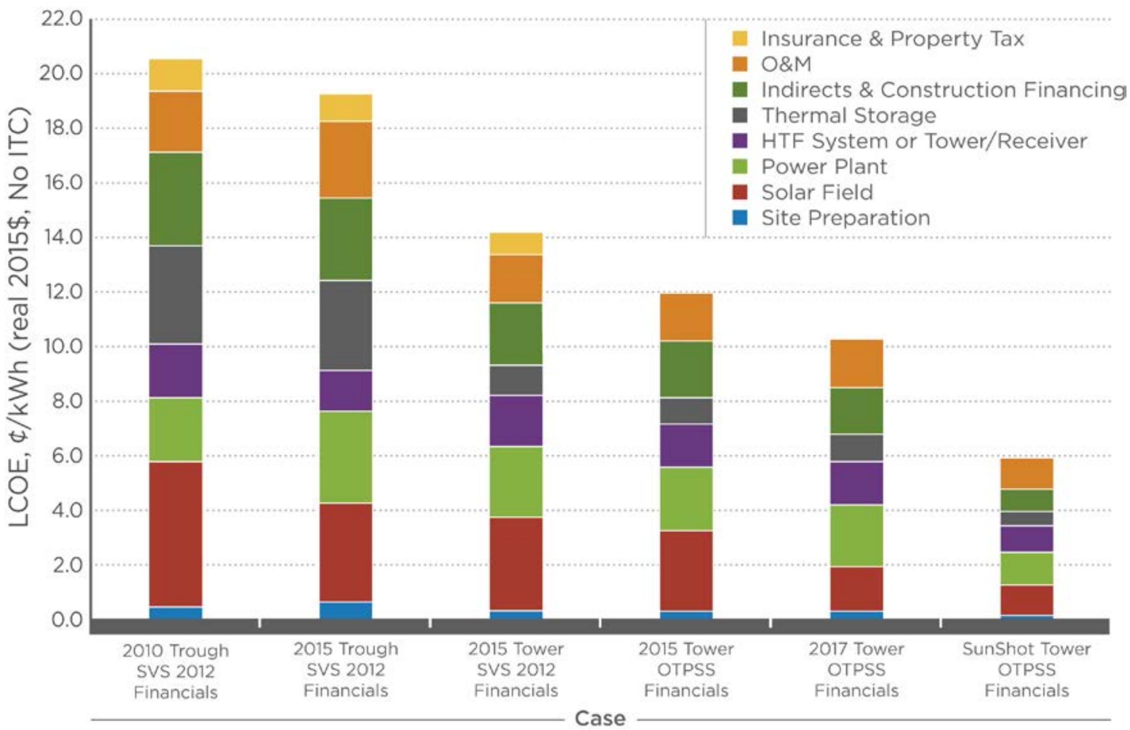


**Figure ES-1. Cost reductions for parabolic trough and tower technologies since the *SunShot Vision Study***

SVS = *SunShot Vision Study* (DOE 2012)
OTPSS = *On the Path to SunShot*

Although the costs for troughs and towers have declined, CSP acceptance and deployment has been negatively impacted by the declining cost of photovoltaic (PV) technology. This situation can be mitigated when considering the flexibility offered by CSP with thermal energy storage (TES). A recent NREL study compared the combined operational and capacity benefits of CSP with TES relative to PV under varying levels of renewable penetration in California. The analysis found that the value of CSP, compared to variable-generation PV, demonstrated an increase in value of up to 6 cents/kWh under a 40% RPS, as shown in Figure ES-2.

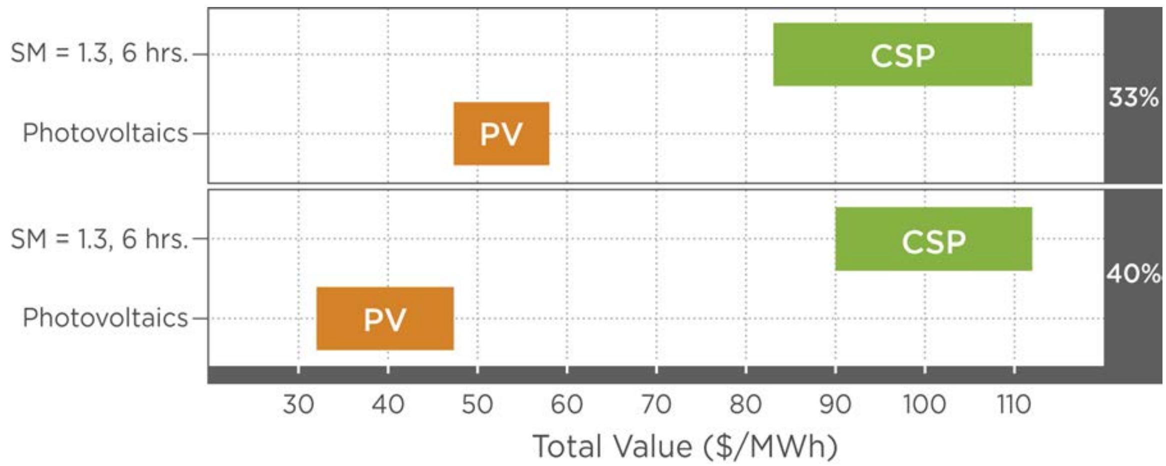


**Figure ES-2. Total value, which includes operational and capacity value, of CSP with thermal energy storage and PV under 33% and 40% RPS scenarios**

SM = solar multiple

This analysis and other similar analyses show that the high grid value of CSP-TES, not just the LCOE, must be considered when evaluating the portfolio of renewable energy technology options. A more comprehensive methodology—an assessment of the *net system cost*—includes comparisons of both costs and grid-wide system benefits of different technologies. The net system cost of a resource represents the difference between the annualized costs of adding a new conventional or renewable generating technology (e.g., CSP-TES, PV, combustion turbines, combined-cycle plant) and the avoided cost realized by displacing other resources providing similar levels of energy and reliability to the system.

Net system costs are shown in Figure ES-3 for three CSP systems representing peaking, intermediate load, and baseload configurations relative to conventional natural-gas-fired combustion-turbine (CT) and combined-cycle (CC) plants offering 1,500 MW of reliable capacity. Figure ES-3 shows that, assuming today's low natural gas prices and carbon emission costs, there is a preference toward choosing a peaking configuration for CSP. However, this decision becomes less clear under a scenario of high natural gas prices and emission costs. In that case, each of the CSP configurations compares very favorably against the conventional alternatives, with systems having intermediate to high capacity factor becoming the preferred alternatives. (Capacity factor is defined as the ratio of actual annual generation to the amount of generation had the plant operated at its nameplate capacity for the entire year.)

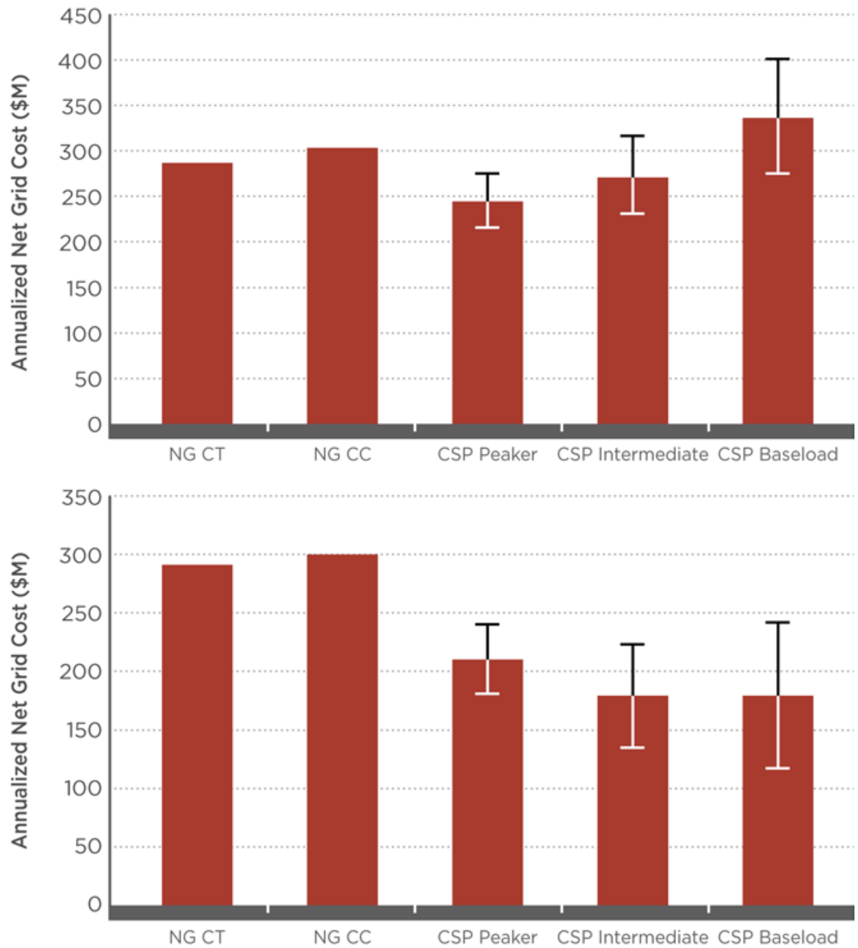


**Figures ES-3. Low natural gas and emission cost scenario (top) and high natural gas and emissions cost scenario (bottom)**

Comparison of net cost for SunShot CSP configurations;
Uncertainty bars represent ±10% variation in SunShot parameters.

Net system costs are similarly shown in Figure ES-4 for three configurations of CSP compared to PV with batteries (where a range of battery costs and lifetime are assumed) and PV with CTs. Each of these technology options provides the same reliable capacity. Figure ES-4 indicates that under current technology costs, the least-expensive option considered is a combination of solar PV and gas CTs, which is not surprising because CSP-TES and grid-scale batteries are relatively immature technologies. These results change when considering future costs. The most optimal configuration of CSP is lower cost than the range of PV-plus-battery costs considered.

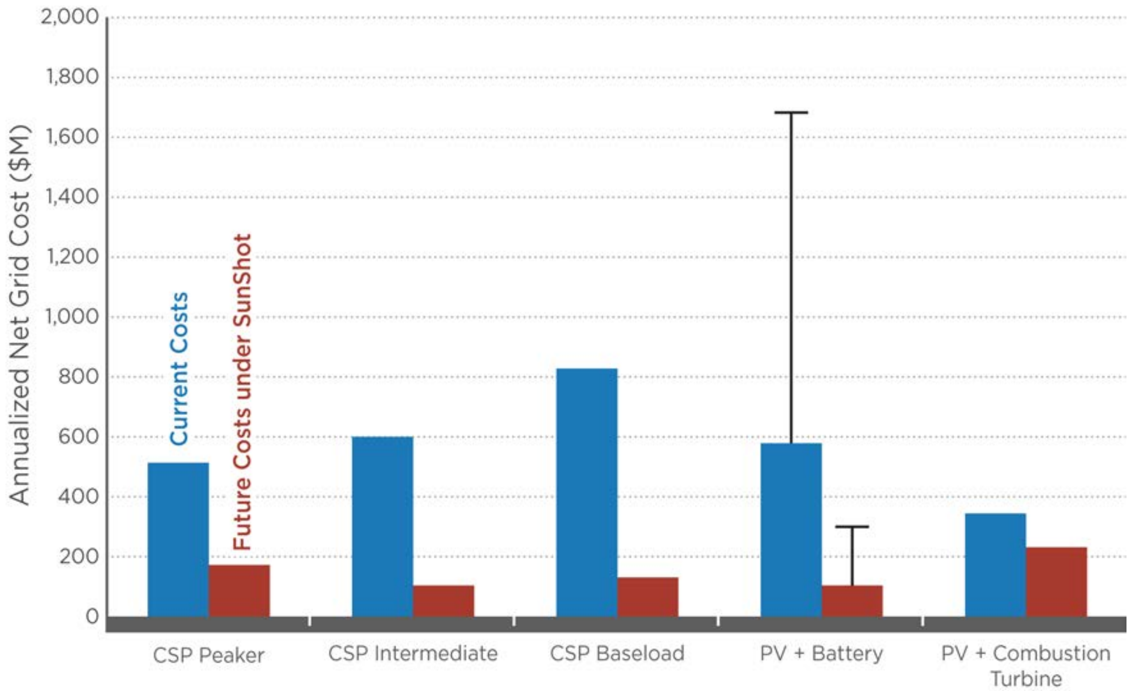


**Figure ES-4. Annualized net cost results for analysis of current and future cost scenarios for CSP, PV with batteries, and PV with combustion turbines**

CSP peaker, intermediate load, and baseload configurations are identical to those shown in Figure ES-3.

# Table of Contents

# List of Figures

# List of Tables

# 1 Introduction

Concentrating solar power (CSP) is well on the path to reaching the U.S. Department of Energy's SunShot Initiative goal of 6 cents/kWh by 2020. In this report, we revisit the original plan for reaching this objective and identify factors related to the market and the technology that have changed. The *SunShot Vision Study* (DOE 2012) focused solely on high-capacity-factor baseload systems to achieve a 6 cents/kWh target, whereas in this report we investigate alternative CSP configurations that can meet the changing needs of the U.S. electricity market. We describe progress made toward achieving U.S. Department of Energy's CSP subprogram's SunShot cost and performance targets and the unique value that CSP can provide to the U.S. energy portfolio.

The primary value that CSP provides to an energy portfolio is its flexibility due to the technology's ability to store thermal energy. Unlike photovoltaics (PV), which generates electricity directly from the sun, CSP plants use mirrors to focus sunlight and produce high-temperature thermal energy that can be stored inexpensively. This feature allows CSP to be a dispatchable electricity resource available whenever there is customer demand, including at times when the sun is not shining. CSP with thermal energy storage (or CSP-TES) thus provides considerable flexibility, increasing its own value to the grid and even enabling greater grid penetration of variable-generation technologies such as PV and wind.

This report is divided into the following sections. Section 2 describes the markets that were anticipated for CSP at the start of the SunShot Initiative in 2011, the subsequent growth of the CSP market, and the market challenges and opportunities predicted to be present at various points in the future. Section 3 provides an overview of the various CSP technologies, the key technical challenges and barriers facing each of these systems, and the anticipated technology improvements that will address these technical challenges. Section 4 discusses cost reductions for the two most widely deployed CSP technologies—parabolic troughs and power towers—since the *SunShot Vision Study* (DOE 2012) was published. This discussion is presented in the context of remaining performance improvements and cost reductions necessary to meet the SunShot objective for cost competitiveness, without subsidies, by 2020. Finally, Section 5 presents new analyses that quantify operational and capacity savings in regional markets for a range of CSP configurations, from peaker to baseload—comparing existing and developing technologies that can meet these market needs against CSP costs based on achieving SunShot's cost and performance targets.

# 2 CSP Markets, Challenges, and Opportunities

## 2.1 CSP Markets

Since the *SunShot Vision Study* (DOE 2012) was published, global deployment of CSP has increased threefold to 4,500 MW, with a similar increase in operational capacity to 1,650 MW within the United States. As shown in Figure 1, CSP capacity has grown significantly since 2009 (IEA 2014). This growth has been particularly concentrated in Spain and the U.S., although other countries began increasing CSP capacity at a greater rate starting in 2013. During this period, annual CSP investments increased by nearly 280% to $6.9 billion.

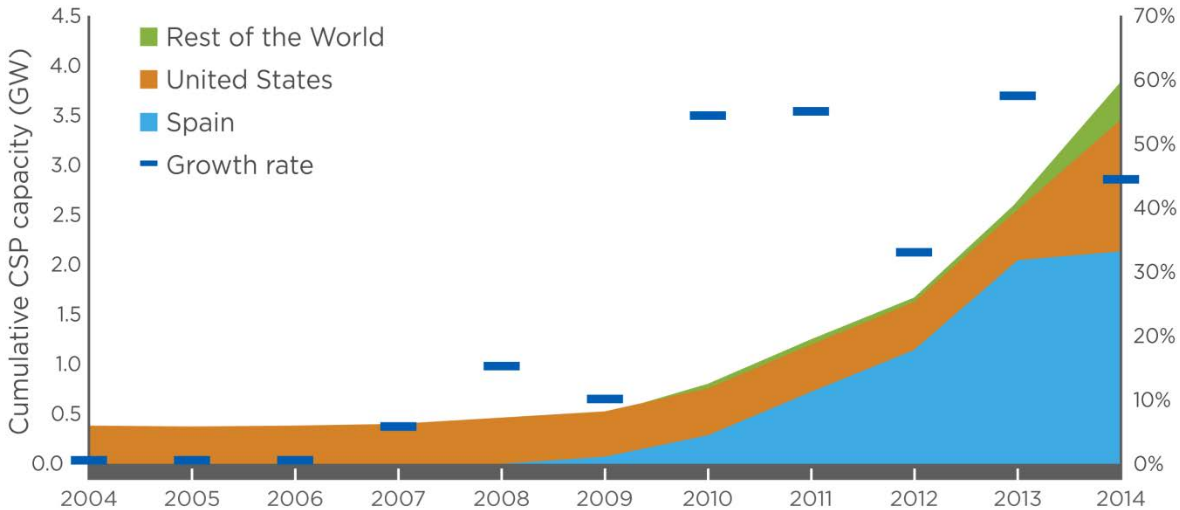


**Figure 1. Global cumulative growth of CSP capacity**

Source: IEA 2014

Growth in U.S. CSP capacity has primarily been driven by policy support at the state and federal levels. State-driven renewable portfolio standards (RPSs), combined with a 30% federal investment tax credit (ITC) and federal loan guarantees, provided the opportunity for CSP developers to kick-start construction of CSP plants throughout the Southwest. New projects supported by these policies include Abengoa's 250-MW Solana and 250-MW Mojave Solar One parabolic trough plants, Next Era's 250-MW Genesis parabolic trough plant, BrightSource's 377-MW Ivanpah direct-steam power tower plant, and SolarReserve's 110-MW Great Dunes molten-salt power tower plant. Although the past three years have seen robust deployment of CSP in the U.S., the current 30% ITC for solar technologies was scheduled to expire at the end of 2016 (Roth 2014), which dampened immediate CSP investments because of the length of time required to permit and construct a CSP plant; plant construction alone typically requires two years, thus dictating that any CSP plant currently under construction could not be completed in time to meet the 2016 deadline. However, at the end of 2015, the U.S. extended the 30% credit through 2019 followed by a gradual two-year decline to 10% (SEIA 2015). The legislation also allows for solar projects to claim the credit for the year in which they begin construction. At this time, it is not clear whether the ITC extension will have an impact over the next few years.

The Spanish market for CSP was driven by a favorable feed-in tariff (FIT), under Royal Decree 436/2004 and Royal Decree 661/2007, which created an ideal environment to develop renewable energy "special regime" projects. With 50 operating CSP plants, dominated by parabolic trough technology, Spain is the only country where CSP is "visible" in national statistics—with close to 2% of annual electricity coming from CSP plants (REE 2014). Maximum instantaneous contribution in 2013 was 7.6%, maximum daily contribution was 4.6%, and maximum monthly contribution was 3.6% (Hoeven 2014). Unfortunately, Spain has recently changed its incentive structure for solar technologies, including retroactively reducing the FIT promised to operating PV and CSP plants. This change has effectively placed a moratorium on new CSP plant construction, and there is no new capacity projected to be built in Spain in the near term.

Beyond the U.S. and Spain, CSP plants of varying configurations and technology types—including troughs, towers, linear Fresnel, and hybrid integrated solar combined-cycle systems (ISCCS)—are operating, under construction, or under development throughout the world. Emerging markets for CSP include the MENA (Middle East and North Africa) region, South Africa, Chile, Australia, and China. Each is pursuing aggressive renewable adoption goals that include CSP deployment. Given the challenges of developing CSP in both the U.S. and Spain, most CSP companies within and outside the U.S. have shifted their attention and resources toward these developing markets. Figure 2 shows a map of the world that highlights the cumulative CSP capacity by country broken out as operational, under construction, or being developed, and a brief overview of markets is provided below.

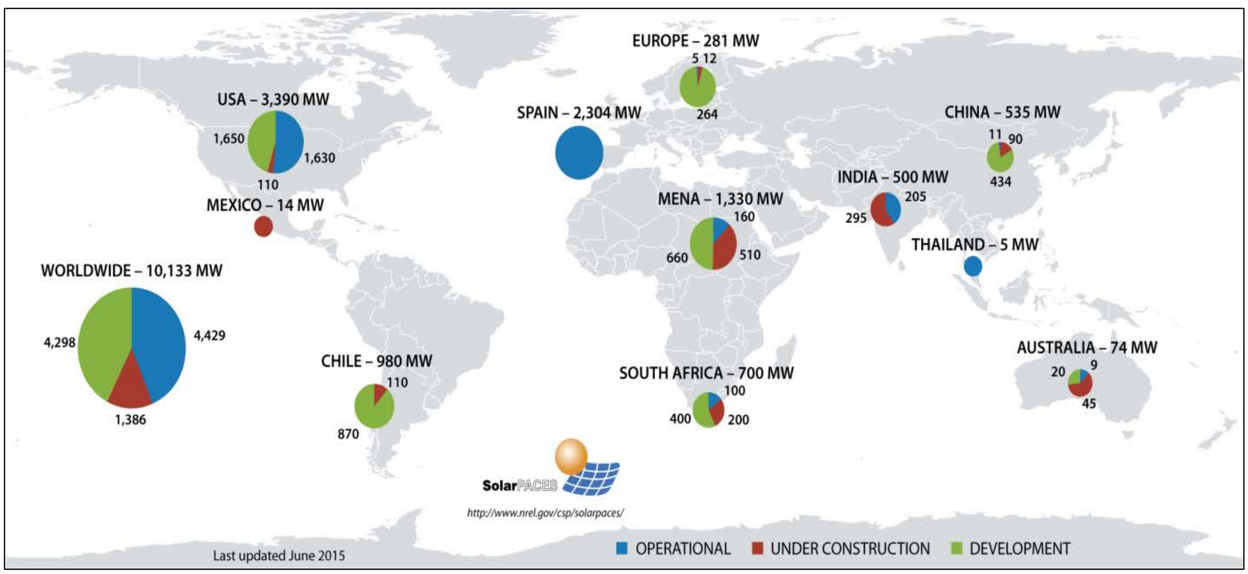


**Figure 2. Cumulative CSP capacity by country and status (operational, under construction, development)**

Source: SolarPACES

### 2.1.1 Africa

South Africa has a target in place of 10,000 GWh of renewable generation through its Renewable Energy Independent Power Producer Procurement Program (REIPPP). Within the program, 4,000 MW of installed capacity is anticipated to be operational by 2030 although considerably more capacity is possible if CSP costs continue to fall. Due in part to attractive time-of-day pricing (the REIPPP includes a revenue multiplier of 2.7 for generation during peak hours), South Africa remains one of the most active markets for CSP—with 100 MW of parabolic trough capacity in operation, 300 MW under construction in 2015 which also includes power towers, and 200 MW in the process of securing financing in order to begin construction. Neighboring Namibia is currently considering both trough and power tower capacity options to its small national grid; initial studies have also been done for Botswana.

In Northern Africa, Morocco has a cumulative parabolic trough and linear Fresnel reflector capacity of 510 MW under construction. Egypt and Algeria both have about 20 MW of parabolic trough systems as part of ISCCS plants, which are one of several possible concepts to hybridize CSP with conventional power-plant technology. Large, mainly European-driven initiatives are pursued to develop the enormous solar potential of this region for the benefit of its own growing economies and a potential future connection to supply clean electricity to Europe (Mediterranean Solar Plan, DESERTEC). However, large deployments have yet to be achieved, in part due to the political turmoil of the "Arabian Spring."

### 2.1.2 Australia

In Australia, Vast Solar previously constructed and operated three CSP research and demonstration facilities. It is currently constructing the Jemalong Solar Thermal Pilot Plant, a 6-$MW_{th}$ power tower electricity generation pilot facility. The pilot will be equipped with 3 hours of TES, and once completed, it will be Australia's only operating, grid-connected CSP plant with TES. Vast Solar is also pursuing plans for a commercial-scale 30-MW CSP plant with 4 hours of TES in the Forbes region. This plant will include about 90 solar array modules and a 30-meter-high tower with a thermal receiver. The completed field is planned to have 65,000 heliostats.

### 2.1.3 Chile

Abengoa has secured funding to develop two 110-MW power tower plants in Chile (HELI-SCP, Dec. 2014). The first plant, already under construction, will use molten-salt technology to store energy for up to 18 hours (Woods 2014). SolarReserve is also planning a 260-MW power tower project in Chile that includes two 130-MW concentrated power towers co-located with a 150-MW PV plant. SolarReserve has expressed interest in increasing this capacity to 800 MW of total CSP and PV capacity (HELI-SCP, Jan. 2015). Reported projections for parabolic trough, power tower, and linear Fresnel reflector CSP capacity in Chile are up to 1,900 MW operational by 2024.

### 2.1.4 China

Through China's 13th five-year plan, the country aims to have 10 GW of CSP capacity installed by 2020. As announced at the end of September 2015, a total capacity of 1 GW of parabolic trough, dish/Stirling, and power tower pilot projects will be confirmed by the end of 2015. BrightSource Energy recently announced an agreement to form a joint venture with Shanghai Electric Group to build power tower plants in China. The joint venture's first proposal is to construct two 135-MW CSP tower plants. According to various articles, SolarReserve is also participating in the Chinese market with power tower systems (HELI-SCP, Nov. 2015).

### 2.1.5 India

India launched the Jawaharlal Nehru National Solar Mission in 2010 with an ambitious goal of deploying 20 GW of solar capacity by 2022. The Mission was divided into three phases: the first phase lasting through 2013, the second phase spanning 2013 to 2017, and the third phase occurring from 2017 to 2022. In the first phase, seven CSP proposals were selected, totaling 470 MW; in 2015, only 200 MW out of the total capacity allocated had entered into operation, which includes power towers, linear Fresnel reflectors, and parabolic trough technologies.

### 2.1.6 Israel

Israel has begun construction on the first 125-MW phase of a planned 250-MW CSP development in the Negev desert. The Ashalim B power tower plant will be built by Megalim Solar Power, BrightSource Energy, and Israel's NOY Infrastructure & Energy Investment Fund (Bayer 2014). The second CSP project at the site, Ashalim A, is a 125-MW parabolic trough plant with 4 hours of thermal energy storage under development by Negev Energy, a joint venture between Shikun & Binui and Abengoa.

### 2.1.7 Saudi Arabia

Saudi Arabia has announced plans to spend $109 billion on more than 50 GW of renewable energy by 2040—of which 25 GW is expected to come from CSP. The country is currently in the planning and development stage for its 50-MW ISCCS Duba 1 plant, and it recently announced the approval of a second 50-MW ISCCS plant.

### 2.1.8 United Arab Emirates, Arabian Peninsula

Abu Dhabi was the first country in the region to build a 100-MW parabolic trough CSP plant, Shams1, which has operated since 2013 under the harsh conditions of a sand desert location. Shams 1 typically operates in a hybridized mode with support from natural gas. Kuwait recently began construction on a 50-MW parabolic trough plant.

### 2.1.9 Other Countries

Other countries that have one or more projects in the few-MW scale include Mexico, Thailand, France, Italy, Germany, Turkey, and Canada.

## 2.2 The Challenge for CSP

Substantial changes to energy markets and energy technologies during the last few years have increased market uncertainty for the global CSP market and impacted growth projections. A manifestation of this uncertainty is the reduction in previous estimates of global CSP growth (IEA 2014), where the global growth rate decreased from about 60% in 2013 to 45% in 2014. Projections still remain substantial in most regions post-2020.

Although CSP growth in the U.S. appears to be positive—with increased capacity having been constructed by companies such as Abengoa, Next Era, BrightSource, and SolarReserve—these projects have been years in the making, and most of the remaining CSP projects that had been under development in the U.S. have been abandoned. Examples include Palen Solar Holdings, which withdrew its petition to develop a 250-MW plant after being approved by the California Energy Commission (CEC), as well as BrightSource, which withdrew its plans to develop a 750-MW installation in Riverside, California. Similarly, considerable doubt exists about SolarReserve's planned Rice Solar Energy Project, also in Riverside, California, because of difficulties in raising project funding. Overall, many of the current projections for the U.S. push further CSP development out a decade or more, with factors that play a critical role in increased deployment including significantly increased variable renewable penetration into the U.S. market and CSP's ability to provide inexpensive energy storage (IRENA 2013).

To a large extent, the declining cost of PV has impacted CSP acceptance and deployment. As shown in Figure 3 (Hill 2015), U.S. PV costs have declined rapidly since 2008. Although CSP costs have also declined significantly during this period, the pace of decline has not matched that of PV. This has been a major factor influencing several large U.S. projects to transition from CSP to PV technologies.

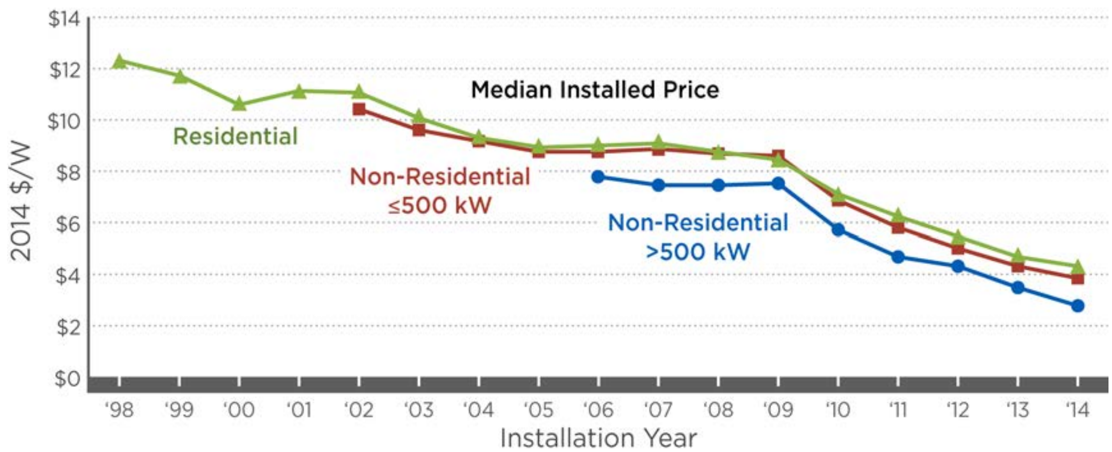


**Figure 3. Falling prices of PV in 2014 dollars per watt for residential and non-residential markets**

## 2.3 The Opportunity for CSP

As previously stated, the cost of PV has recently declined at a more rapid rate than the cost of CSP-TES. However, the flexibility offered by CSP-TES is a key differentiator from variable renewables such as PV and wind. As described earlier, CSP-TES is highly dispatchable and generally less variable in output than traditional solar PV due to the presence of storage and thermal inertia (Denholm et al. 2013). Because of the ability to inexpensively integrate storage, CSP-TES offers considerable benefits to regional grids by supporting both the system operators and load-serving entities.

It is important to evaluate several potential benefits when assessing the value of CSP-TES relative to alternate renewable energy resources such as PV and wind. CSP provides multiple benefits, including dispatchable high-value energy, operating reserves, and reliable system capacity. The dispatchability of CSP results in energy production during periods of highest demand, offsetting the most costly (and often highest emissions) fossil generators. CSP can also ramp rapidly, providing multiple ancillary services such as regulation and spinning reserves. Figure 4 describes the operational benefit (primarily avoided fossil generation) for a number of

CSP configurations of various solar multiples (SM) and storage capacities (Jorgenson et al. 2014). The SM is a measure of the ratio of the size of the solar field to the designed size of the power block. As seen from the figure, the greatest system benefit occurs at lower SM plants that predominately displace high-cost generation from inefficient combustion turbines.

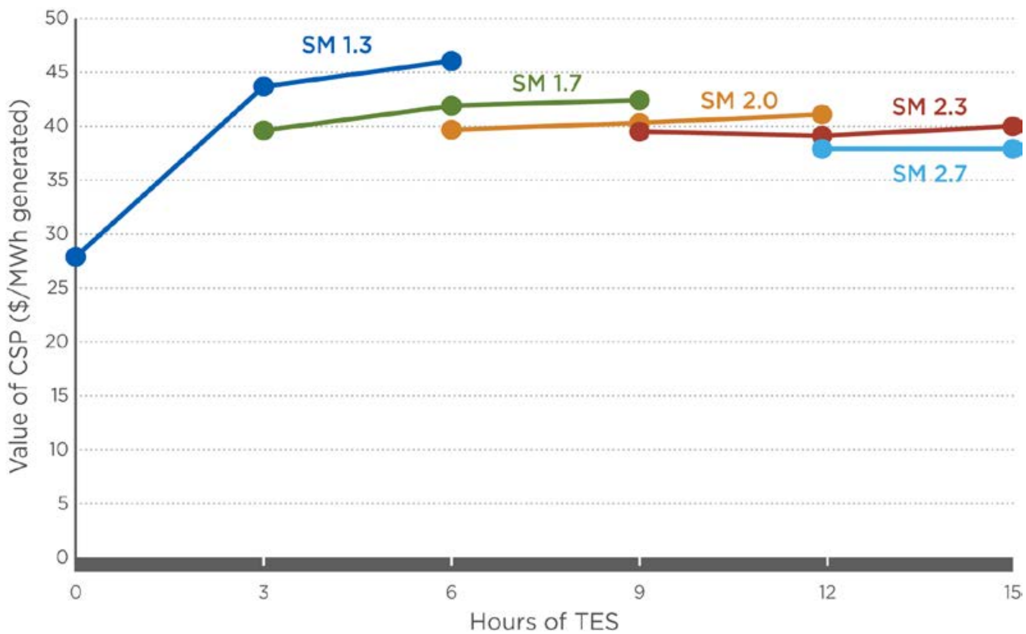


**Figure 4. Marginal operational value of tower CSP-TES plants with varying configurations in California**

As the amount of variable wind and PV on the grid increases, the demand for flexible generation resources will likely increase. Greater amounts, as well as new types, of operating reserves may be needed. As an example, several regions of the U.S. are in the process of introducing a flexibility/ramping reserve product well suited to CSP (Denholm et al. 2016). Another product being considered for the reserve market is a frequency-responsive reserve. Previous analysis has demonstrated the ability of CSP to provide frequency-response reserves that can help maintain grid stability (Miller et al. 2014); however, the economic value of grid-stability services provided by CSP has yet to be evaluated in detail.

Another significant benefit of CSP-TES is its ability to provide firm capacity, which is capacity available to the power system at times of greatest need, which are most often the hours of highest net demand (Madaeni et al. 2011; Jorgenson et al. 2014). Variable-generation resources such as PV and wind tend to be limited in availability during these hours at high penetration of renewables on the grid because these hours typically occur when the solar or wind resources are unavailable (Mills and Wiser 2012). As a result, installation of these technologies alone cannot meet system peak demand, especially as older fossil plants are retired and new capacity additions become necessary to maintain system reliability.

Analysis performed by the National Renewable Energy Laboratory (NREL) indicates that once PV penetrations achieve 15% within California, the capacity credit earned by PV can be less than 10% (Jorgenson et al. 2015). Capacity credit represents the percentage of nameplate capacity that can be considered reliable and available during times of system need. Other studies indicate a similarly low capacity credit when high levels of penetration are analyzed (Mills and Wiser 2012). On the other hand, CSP-TES offers considerably more reliability to the grid. The capacity credit of CSP-TES can be estimated by taking into account the plant's ability to provide needed electricity output during the 100 hours of highest net load (Tuohy and O'Malley 2011; Jorgenson et al. 2014). Both the amount of TES and the solar multiple affect the ability of a CSP-TES plant to provide reliable energy. Table 1 shows the capacity-credit results for a subset of solar multiples and thermal storage capacities (Jorgenson et al. 2015). Configurations with less than six hours of energy storage capacity would result in lower capacity credit (Sioshansi et al. 2014). The flexibility of CSP should also allow it to meet "flexible capacity" requirements, such as the California Public Utility Commission (CPUC) requirement that all load-serving entities under its jurisdiction—primarily the three large investor-owned utilities in the state—procure capacity with sufficient flexibility to address the largest predicted 3-hour ramp rate in each month (CPUC 2014).

**Table 1. Capacity Credit (%) for Various Configurations of CSP-TES**

| | Solar Multiple | | | | | | |
|---|---|---|---|---|---|---|---|
| **TES (hours)** | **0.7** | **1.0** | **1.3** | **1.7** | **2.0** | **2.5** | **3.0** |
| 6 | 93% | 96% | 97% | 98% | 98% | – | – |
| 9 | – | – | – | 98% | 98% | 99% | – |
| 12 | – | – | – | – | – | 99% | – |
| 15 | – | – | – | – | – | 99% | 99% |
| 18 | – | – | – | – | – | – | 99% |

Figure 5 describes the result of a recent NREL study comparing the combined operational and capacity benefits of CSP-TES relative to PV under varying levels of renewable penetration in California (Jorgenson et al. 2014). The analysis found that the value of CSP, compared to variable-generation PV, demonstrated an increase in value of up to 6 cents/kWh under a 40% RPS.

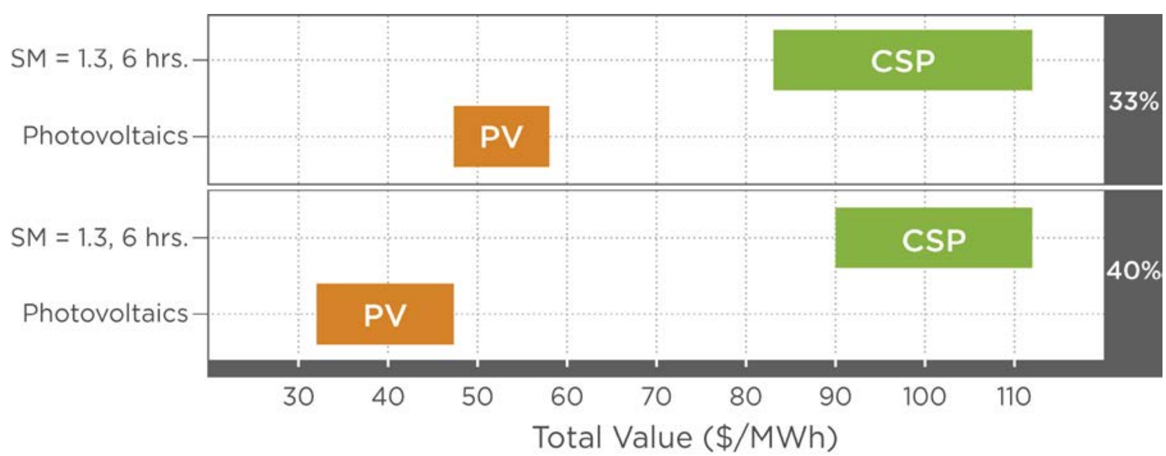


**Figure 5. Total value, which includes operational and capacity value, of CSP-TES and PV under 33% and 40% RPS scenarios**

SM = solar multiple; hours indicate TES

These analyses show that grid value—not only the capital cost—is a necessary consideration when evaluating a portfolio of renewable energy technology options. However, even with this more appropriate evaluation methodology, large-scale CSP deployment will ultimately require continued reductions in the capital cost of CSP systems relative to today's technology. The next section overviews the primary types of CSP systems in use today and the key technical challenges and barriers for each technology, and it describes ongoing and anticipated technology improvements envisioned to address the identified technical challenges.

# 3 CSP Technologies

## 3.1 Overview of CSP Systems

### *3.1.1 Parabolic Trough*

Parabolic trough systems are the most mature type of CSP technology, representing the majority deployed capacity throughout the world. Parabolic trough power plants consist of large fields of mirrored parabolic trough collectors and receivers, a heat-transfer fluid (HTF)/steam-generation system, a thermoelectric conversion system such as a Rankine steam turbine/generator, and have the option of including TES. The use of TES results in both dispatchable generation and higher annual generation per unit of capacity, although the larger collector field and storage system lead to higher upfront capital investment. Trough solar fields can also be deployed in conjunction with fossil-fueled power plants to augment the steam cycle, which can improve performance of the overall system by lowering the heat rate of the plant and either increasing power output or displacing fossil-fuel consumption.

The solar field consists of large modular arrays of single-axis-tracking solar collectors arranged in parallel rows, usually aligned on a north-south horizontal axis. Each solar collector has a linear parabolic-shaped reflector that focuses the incident solar radiation onto a linear receiver (absorber tube) located at the focal line of the parabola (Figure 6). The collectors track the sun from east to west during the day and the HTF, typically a synthetic oil, is heated within the receiver tubes to a temperature of about 390 °C, which is the upper limit of the thermal stability of the HTF. Once heated, the HTF flows through a heat exchanger to either generate high-pressure superheated steam (typically 100 bar at 370 °C), or, if the system includes TES, heat up molten salt. Once steam has been generated, it is fed to a conventional reheat steam turbine/generator to produce electricity. The spent steam from the turbine is condensed in a standard condenser and returned to the heat exchangers via condensate and feed-water pumps to be recycled back through the system. Wet, dry, or hybrid cooling towers can be used for heat rejection from the condenser, with the selection of cooling technology impacting water use, cycle performance, and cost. Figure 7 is a schematic of a trough plant with a fossil-fuel-fired backup boiler and TES—similar to the Solana Generation Station in Arizona, currently the world's largest parabolic trough plant that has a 280-MW gross capacity and 6 hours of thermal storage using molten salt (Figure 8).

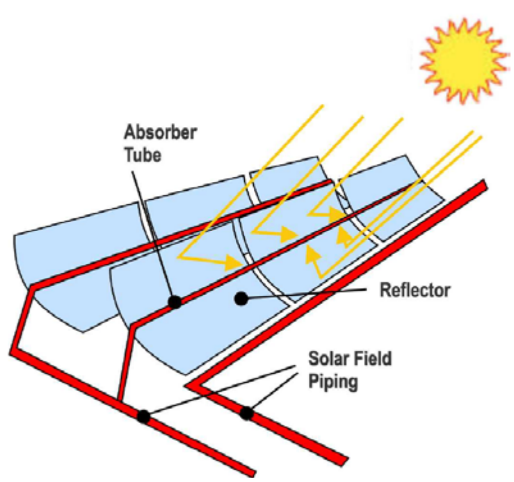


**Figure 6. Parabolic trough components**

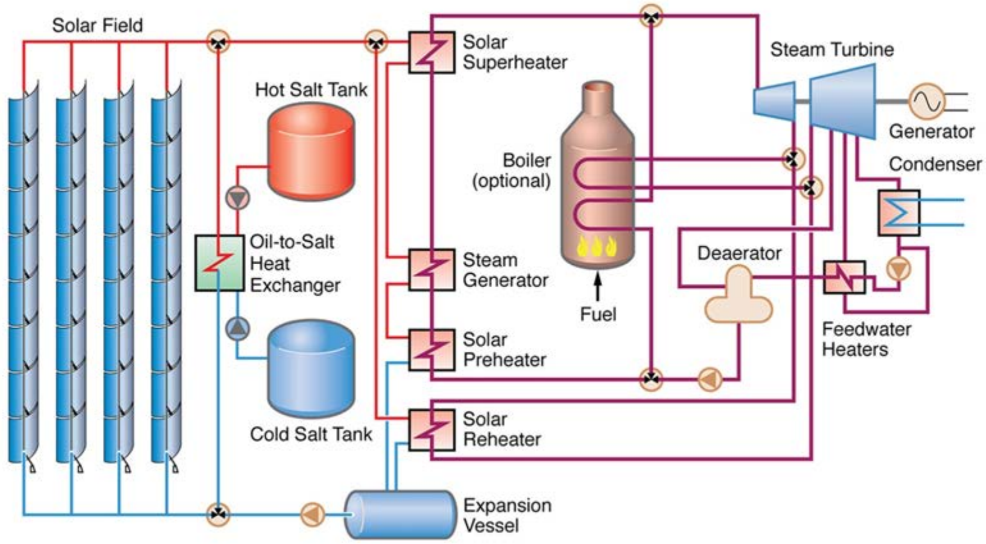


**Figure 7. Parabolic trough plant with indirect two-tank thermal storage and fossil-fuel backup system**

Source: EPRI 2010

**Figure 8. Solana Generating Station in Gila Bend, Arizona, which is currently the world's largest parabolic trough plant**

Photo from Abengoa Solar

The design-point solar-to-electric efficiency is defined as the net efficiency in the ideal case when the sun is directly overhead. Currently, for a parabolic trough plant, it ranges from 24%–26%, and the overall annual average solar-to-electric conversion efficiency is about 13%–15%, where the solar input is defined by the direct normal irradiance (DNI). The design-point values represent an ideal case that is useful for making comparisons between different components, such as two different receiver designs. The annual average efficiency provides a better assessment of expected actual operation than does the design-point efficiency.

### 3.1.2 Power Tower

Central-receiver systems such as solar thermal power-tower plants can achieve higher-temperature operation when compared to parabolic trough systems. This higher temperature can yield higher thermal-to-electric conversion efficiencies in the power block and lower costs for storage. Power towers use heliostats—reflectors that rotate about both the azimuth and elevation axes—to reflect sunlight onto a central receiver. A large power-tower plant can require several thousand to more than 100,000 computer-controlled heliostats that track the sun. Heliostat size, weight, manufacturing volume, and performance are important design variables, and developers have selected different approaches to minimize cost. For example, some heliostat technology can be installed on relatively uneven land, with 5% or more slope, thereby reducing site-preparation costs for new projects.

Currently, the two principal power-tower technology concepts pursued by developers are defined by the type of HTF in the receiver: steam or molten salt. In direct-steam power towers, heliostats reflect sunlight onto a receiver on a tower. The receiver in a direct-steam power tower is similar in function to a boiler in a conventional coal-fired power plant. The feed water, pumped from the power block, is evaporated and superheated in the receiver to produce steam, which is then fed into a turbine/generator to generate electricity. Current steam conditions for direct-steam towers range from saturated steam at 250 °C to superheated steam at over 550 °C. Several characteristics of direct-steam power towers make them attractive: their straightforward design; use of conventional boiler technology, materials, and manufacturing techniques; high thermodynamic efficiency; and low parasitic power consumption. Short-duration direct-steam/water storage has been demonstrated at the 20-MW PS20 tower in Spain. Like many CSP technologies, steam towers can be hybridized with natural gas to provide additional operating flexibility and enhanced dispatchability. Figure 9 shows photos of the Ivanpah Solar Electric Generating System, which consists of three direct-steam power towers and more than 170,000 heliostats (each 15 $m^2$), with a gross capacity of 390 $MW_e$.

**Figure 9. Ivanpah Solar Electric Generating System, which employs direct-steam heating in the receiver**

Source: BrightSource Energy

In a molten-salt power tower, salt at a temperature of about 290 °C is pumped from a cold storage tank to a receiver, where concentrated sunlight from the heliostat field heats the salt to about 565 °C. The salt is typically a blend of sodium and potassium nitrate, which are ingredients sold commercially as fertilizer. The hot salt is held in a storage tank, and when electric power generation is required, hot salt is pumped to the steam generator to produce high-pressure steam at nominal conditions of 100–150 bar and up to 540 °C. The now-cooler salt from the steam generator is returned to the cold-salt storage tank to complete the cycle. The steam is converted to electrical energy in a conventional steam turbine/generator. By placing the storage between the receiver and the steam generator, solar energy collection is decoupled from electricity generation. Thus, passing clouds that temporarily reduce sunlight do not affect turbine output. In addition, the TES may be less than half the cost of salt TES in trough plants because the larger temperature range across the storage system enables more energy to be stored per mass of salt. The combination of salt density, salt specific heat, and temperature difference between the two tanks allows economic storage capacities of up to 15 hours of turbine operation at full load. Such a plant could run 24 hours per day, 7 days per week in the summer and part-load in the winter to achieve a 70% solar-only annual capacity factor. The 20-$MW_e$ Gemasolar plant in

Spain is designed for such performance, whereas the 110-$MW_e$ Crescent Dunes molten-salt power tower in Nevada is designed for 10 hours of storage (Figure 10).

**Figure 10. 110-$MW_e$ Crescent Dunes Solar Energy Project in Tonopah, Nevada, with ten hours of thermal storage**

Source: C. Ho, SNL

The annual average solar-to-electric conversion efficiency of a power tower is about 14%–18%, with direct-steam towers slightly higher than molten-salt towers. The design-point efficiency is about 20%–24%. As discussed for troughs, annual average efficiency represents overall real-world performance, whereas design-point values are useful for comparing the performance of individual components. The choice of wet, dry, or hybrid cooling towers can influence water use, cycle performance, and cost.

### *3.1.3 Linear Fresnel Reflector*

Linear Fresnel reflectors (LFRs) approximate the parabolic shape of a traditional trough collector with long, ground-level rows of flat or slightly curved reflectors that reflect the solar rays toward an overhead stationary linear receiver. Flat reflectors and fixed receivers lead to lower capital costs relative to a traditional trough-based plant, but LFR plants are less efficient on a solar-to-electricity basis. Superheated steam at about 380 °C has been demonstrated in an LFR plant, and there are proposals for producing steam at 450 °C to enable higher power-cycle efficiency. Compact LFR technology uses a design with two parallel receivers for each row of reflectors. This configuration minimizes blocking of adjacent reflectors and reduces required land area. Another advantage is that, depending on the position of the sun, the reflectors can be alternated to point at different receivers, thus improving optical efficiency (Figure 11).

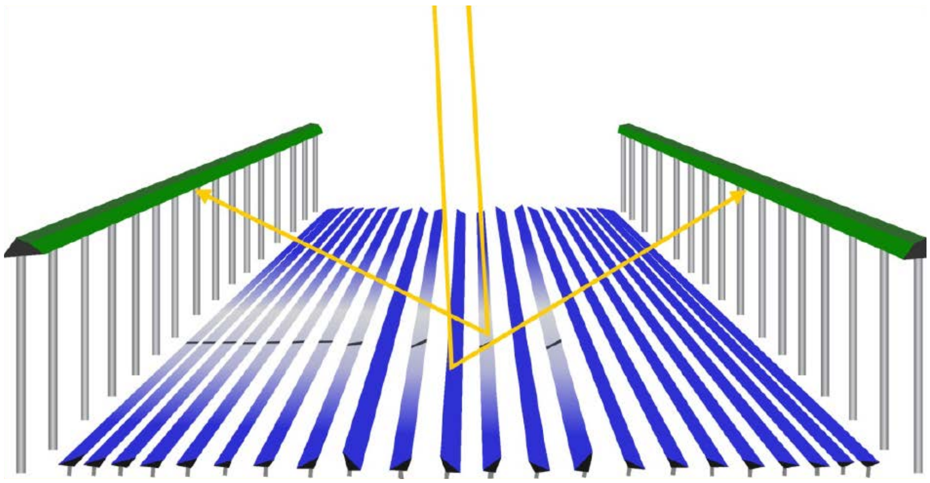

**Figure 11. Compact linear Fresnel system**

### *3.1.4 Dish/Engine System*

Dish/engine CSP systems use a collection of reflectors assembled in the shape of a parabolic dish to concentrate sunlight onto a receiver cavity at the focal point of the dish. Within the receiver, the heater head collects this solar energy and runs an engine-driven generator to produce electricity. Similar to heliostats, all dishes rotate along two axes to track the sun for optimum capture of solar radiation. The three major types of engines used at the core of dish/engine technology are kinematic Stirling engines, free-piston Stirling engines, and Brayton turbine-alternator-based engines. Dishes have also been proposed with air receivers that feed hot air to a steam generator. Both kinematic and free-piston Stirling engines harness the thermodynamic Stirling cycle to convert solar thermal energy into electricity by using a working fluid such as hydrogen or helium. Brayton systems use turbine-alternator engines with compressed hot air to produce electricity. Dish/Stirling systems generate 3–30 kW of electricity, depending on the size of the dish and type of heat engine used. Dish/Brayton systems have been proposed at sizes up to 200 kW. Two types of dish/engine systems are shown in Figure 12.

**Figure 12. Two types of dish/engine systems**

Sources: left image, Stirling Energy Systems 2010; right image, Infinia 2010

Some dish/engine technology can be installed on relatively uneven land—with 5% or more slope—thereby reducing the cost of site preparation for new projects. Dish/engine systems are cooled by closed-loop systems, similar to an automobile engine; this type of cooling, combined with the lack of a steam cycle, endow these systems with the lowest water use per megawatt-hour among all the CSP technologies. As a modular technology, dish/engine systems are built to scale to meet the needs of each individual project site, potentially satisfying loads from kilowatts to gigawatts. This scalability makes the dish/engine technology applicable for both distributed and utility-scale generation. Dish/Stirling systems have demonstrated the highest-recorded CSP design-point solar-to-electric efficiency of 31.4% and have an estimated annual conversion efficiency in the low-20% range. Despite its high efficiency, few dish/Stirling commercial systems have been deployed due to this technology's relatively higher costs. In addition, the lack of thermal storage in current dish systems means that the dishes, although modular, are in direct competition with PV systems, which have benefitted from significant cost reductions in recent years. The U.S. Department of Energy (DOE) has recently funded research to provide several hours of storage on dish systems in an attempt to increase the capacity factor and reduce the levelized cost of dish/engine systems.

## 3.2 CSP Components—Challenges, Barriers, and Technology Improvement Opportunities

The following sections describe the major components of a CSP plant, along with associated features, challenges, and barriers. We also present technology improvement opportunities that have been pursued by DOE to increase performance and reduce costs and/or risks. Table 2 summarizes key cost and performance goals for 2020 that have been set by DOE.

**Table 2. Goals Established by DOE for Various Components of CSP Plants**

| Solar Field | Receiver | Heat Transfer Fluid | Thermal Storage | Power Block |
|---|---|---|---|---|
| Cost<br>≤ $75/m²<br>(Beyond SunShot: ≤ $50/m²) | Cost<br>≤ $150/kW$_{th}$ | Cost<br>≤ $1/kg | Cost<br>≤ $15/kWh$_{th}$ | Cost<br>≤ $900/kW$_{e}$ |
| - Optical error (calm) ≤ 3.0 mrad<br>- Optical error (windy) ≤ 4.0 mrad<br>- Max operational wind speed ≥ 35 mph<br>- Max survivable wind speed ≥ 85 mph<br>- Lifetime ≥ 30 yrs | - Thermal efficiency ≥ 90%<br>- HTF fluid exit temp ≥ 720 °C<br>- Lifetime ≥ 10,000 cycles | - Thermal stability ≥ 800 °C<br>- Melting point ≤ 250 °C | - Power-cycle inlet temp ≥ 720 °C<br>- Exergetic efficiency ≥ 95% | - Net thermal-to-electric cycle efficiency ≥ 50%<br>- Dry-cooled at 40 °C ambient temp |

### 3.2.1 Solar Collectors

Solar collectors for CSP track the sun and concentrate solar energy onto a receiver. The collectors can be configured as single-axis parabolic troughs and linear Fresnel systems or as two-axis heliostats and dish systems. At today's costs for CSP systems, collectors are the most expensive component of a CSP plant, typically constituting about 30%–40% of the plant cost. Therefore, it is important to optimize collector design, performance, and cost. SunShot goals for collector cost and performance include having an optical error ≤ 3 mrad, the ability to survive in wind speeds ≥ 85 mph, a collector lifetime ≥ 30 years, and costs ≤ $75/m^2$.

**Reflectivity and Mirror Cleaning.** The initial reflectivity, long-term durability, and soiling of mirrors has a direct impact on the levelized cost of electricity (LCOE) of CSP plants. Keeping the mirrors clean and highly reflective is a challenge, especially with minimal water usage. For heliostats with long focal lengths, achieving highly specular reflective surfaces is also important.

- DOE has funded passive methods to keep mirrors clean using anti-soiling coatings, as well as low- to no-water cleaning techniques such as transparent electrodynamic screens that can vibrate soil and dust off the mirror surfaces.
- Reflective polymeric films are being researched that may yield lighter-weight reflective materials compared to silvered glass, thereby requiring less robust and less costly drives. Studies have been pursued to combine these films with lightweight rigid-foam supports. At least one developer has successfully integrated a polymer film into a full-scale commercial parabolic trough design.
- Front-surface glass mirrors with protective hardcoats are being studied to yield greater reflectance, and novel glass-molding techniques have been studied to create more-precise mirrors in a variety of shapes.

**Alignment, Focusing, and Tracking.** Accurate alignment and focusing of the mirror facets is critical for collector performance. However, during manufacturing and installation, misalignment and mounting issues can and have caused unforeseen optical errors. Optical errors, poor alignment or focusing, and tracking errors can significantly reduce performance of the collector and overall CSP system.

- DOE has funded several projects to reduce total optical errors to less than 3 mrad (calm winds) and 4 mrad (windy conditions). The recently released Concentrating Optics for Lower Levelized Energy CosTS (COLLECTS) funding opportunity intends to achieve these identical targets at a cost of <$50/m^2$. This new, aggressive cost goal goes beyond the SunShot target.
- New closed-loop control systems using cameras and reflections from the mirrors may improve pointing accuracy and system performance.
- New, rapid characterization methodologies to align and install heliostats with minimal labor have also been studied.

**Spectrum Splitting and Integrated PV Mirrors.** Currently, collectors are used in CSP plants solely to convert sunlight to thermal energy. Mirrors in conventional CSP plants cannot be used to concentrate sunlight under diffuse-sky conditions or when there are significant clouds. In addition, the conversion of sunlight to heat and then to electricity reduces the potential efficiency of a solar-to-electric system.

- The Advanced Research Projects Agency-Energy (ARPA-E) Full-Spectrum Optimized Conversion and Utilization of Sunlight (FOCUS) program has sponsored a number of projects to investigate the use of spectrum splitting and integrated PV within mirrors to produce more-efficient systems that produce both electricity and thermal energy. Low-cost, high-performance PV cells (at higher temperatures) may make integration of PV cells with heliostats and collectors more advantageous, especially under diffuse lighting conditions.

**Drives, Structural Support, and Controls.** The azimuth drive is the most expensive part of the heliostat, and next-generation drives and associated support structures must provide stiffness and optical accuracy under gravity and dynamic wind loads while being inexpensive and light. Accurate tracking is also required to maximize the solar flux on the receiver. Control algorithms, drives, and corrective measures to maintain pointing accuracy is needed, especially at long slant ranges.

- DOE has funded new collector designs and support structures such as space frames and low-profile systems to improve stiffness and optical accuracy under gravity and dynamic wind loads.
- New wireless control systems that can maintain optical accuracy with low cost and power requirements have also been pursued.

**Manufacturing and Installation.** Manufacturing and transporting collectors on-site can increase costs and collector accuracy errors. Complicated or difficult installation procedures can also increase costs.

- Highly automated facilities and equipment to support the low-cost manufacture and installation of heliostats and collectors will lead to cost reduction. The U.S. Department of Energy's Solar Manufacturing Technology (SolarMat) and SunShot CSP funding opportunities have funded projects to improve construction, assembly, and installation methods for heliostat and trough systems to reduce construction time, which, in turn, reduces financial risk and costs.

### 3.2.2 Thermal Receivers

Thermal receivers harness concentrated sunlight from the collectors and convert that sunlight into thermal energy within a heat-transfer material. The heat-transfer media can be a liquid, such as water, synthetic oil, or molten salt; a gas, such as air, helium, or hydrogen; a solid, such as sand or ceramic particles; or a supercritical phase, such as supercritical carbon dioxide. Liquids and supercritical fluids are typically contained and transported within a tubular receiver, whereas gases can be contained in tubes or volumetric (honeycomb-like) receivers. Solid particles can be released into a cavity receiver for direct irradiance or across irradiated tubes as a fluidized bed or moving packed bed. SunShot goals for the receiver include exit temperatures ≥ 720 °C, thermal efficiency ≥ 90%, lifetime ≥ 10,000 cycles, and cost ≤ $150/kW$_{th}$.

**Solar-Selective Coatings.** Receivers should be highly absorptive in the solar wavelengths (~0.4–2.5 micrometers). However, at high temperatures, receivers can emit a significant amount of thermal radiation, thereby losing heat to the environment. At these high temperatures there is an overlap of the spectral absorptance and emittance, making it difficult to develop a truly selective absorber. Additionally, coatings and paints must endure high temperatures in an oxidizing environment for many thermal cycles and under potentially large thermal gradients.

- DOE has funded several solar-selective coating projects to develop robust materials that can provide high solar absorptance (> 94%) and low thermal emittance (≤ 10%). Refractory coatings, use of nanoparticles, and new ceramic/metal composite compositions are possible means to achieve these metrics. New standards for application and curing processes for Pyromark 2500, the current commercial standard, are also being developed.

**High-Temperature Receiver Designs.** Higher receiver temperatures are being sought to enable higher-efficiency power cycles such as supercritical carbon dioxide ($sCO_2$) closed Brayton cycles. However, at higher temperatures, radiative and convective losses from the receiver are increased. Challenges are also posed by heat transfer across walls and surface interfaces during heat-transfer media transportation to the storage system or power block.

- Multi-cavity and microchannel designs are being pursued to increase the available heat-transfer area to high-temperature, high-pressure fluids and media in compact designs, with the goal of reducing heat loss and increasing thermal efficiency.
- Extended heat-transfer surfaces within tubes can increase heat transfer and structural reliability and are being investigated for high-temperature, high-pressure applications such as direct $sCO_2$ receivers.
- The use of a quartz window for cavity receivers can reduce convective heat losses, but potentially at the expense of reflected solar losses. Quartz windows also limit the ability to use pressurized gases and limit the size of the cavity opening.
- Silicon carbide ceramic receivers are being studied for high-temperature, high-pressure applications.
- Particle receivers are being investigated as a means to achieve particle temperatures ≥ 720 °C with direct storage. Different particulate materials and designs have been studied, including direct-heating receivers with free-falling or obstructed particle flows and indirect-heating receivers with fluidized or falling particles flowing across irradiated tubes. Other particle receivers include rotating kilns and vortex reactors.
- Heat pipes are being evaluated as a way to increase the heat transfer from tube or panel surfaces with high surface fluxes to fluids or particles.
- Liquid-metal receivers can yield very high solar fluxes and efficiencies due to the extremely high thermal conductivity of liquid metals (e.g., sodium). DOE has funded research on high-efficiency liquid-metal receivers.

### 3.2.3 Thermal Energy Storage

Incorporation of thermal energy storage is the key advantage of CSP plants and can be used to produce electricity when the sun is not shining. The round-trip efficiency of thermal storage can be very high (≥ 99%), and costs are low relative to alternatives such as battery storage. SunShot goals for thermal storage include power-cycle inlet temperature ≥ 720 °C, exergetic efficiency ≥ 95%, and a cost ≤ $\$15/kW_{th}$.

**Thermochemical Energy Storage.** Storing solar energy in the form of chemical bonds is attractive because the energy can be stored indefinitely and thermal boosting can occur in the form of reduction/oxidation reactions. Kinetics, energy density, and costs present some challenges and limitations to applying thermochemical energy storage.

- The use of perovskites as sand-like particles is being studied as part of the U.S. Department of Energy's Efficiently Leveraging Equilibrium Mechanisms for Engineering New Thermochemical Storage (ELEMENTS) program. These particles may be a means to collect, store, and transfer heat for high-temperature applications using reduction/oxidation reactions.
- Calcium and strontium carbonates are being investigated in endothermic-exothermic chemical reaction cycles.
- Ammonia dissociation and reformation is being evaluated as a means of thermal energy storage with a relatively simple product separation process.

**Phase-Change Materials (PCMs).** The latent heat of phase change can store or retrieve large amounts of energy. However, the process is isothermal, so unless the power cycle relies on nearly isothermal conditions (e.g., Stirling cycle, heavily recuperated $sCO_2$ cycles), high exergetic losses may occur.

- DOE has investigated cascaded PCMs to mimic more exergetically efficient sensible heat-exchange conditions.
- Various encapsulation methods for PCM have been evaluated to address challenges with heat transfer while the system is discharging heat. Examples include encapsulation of small amounts of PCM within a solid that will not undergo phase change and impregnation of PCM into metal or graphite foams.
- The use of PCMs with embedded thermosyphons or heat pipes have been investigated to reduce thermal resistances.

**Solid Particles.** Sand, sintered bauxite, alumina, and ceramics have been investigated as a heat-transfer and storage media. Desirable features include a high solar absorptance (for directly irradiated particles), low thermal emittance, good durability, resistance to sintering, high heat capacitance, ease of flow, and low cost.

- Studies have shown that commercial ceramics particles (sintered bauxite) used as proppants for hydraulic fracturing have many of the desired properties for directly irradiated receivers.
- Silica or alumina particles may work well in enclosed particle receivers because they do not receive direct solar irradiation.

**Molten Salts.** Conventional molten nitrate salts become unstable at ~600 °C, and they freeze at ~228 °C. Achieving higher-temperature, higher-efficiency power cycles requires new higher-temperature compositions. Also, lower freezing-point salts would aid in the mitigation of freezing events.

- DOE has funded projects to investigate deep eutectic or low freezing-point mixtures of inorganic salts.
- Research has been conducted to embed ceramic and silica nanoparticles in molten salt to increase heat capacity.
- Chloride salts have also been investigated as a thermodynamically stable means of achieving higher operating temperatures (> 700 °C).

**Solid-State Sensible Storage.** Solid-state storage systems have been researched due to the relative low cost of many potential solid-state storage media and their ability to achieve higher-temperature operation. Heat transfer into and out of the solid represents the largest challenge in developing these systems.

- DOE has investigated heat storage in large blocks of solid media such as concrete or graphite.
- Packed-bed systems using alumina have been investigated as storage systems for use with gaseous heat-transfer fluids.

### 3.2.4 Power Block

The power block converts thermal energy into electricity using a heat engine (e.g., Rankine cycle, Brayton cycle, Stirling cycle). Exergy losses in heat exchangers, parasitic loads from pumps and fans, and waste heat during cooling contribute to penalties in the thermal-to-electric cycle efficiency. SunShot targets for the CSP power block include a net thermal-to-electric cycle efficiency ≥ 50%, use of a dry-cooling heat sink at 40 °C ambient temperature, and a cost ≤ \$900/kW$_e$.

**s$CO_2$ Brayton Cycles.** DOE is pursuing supercritical carbon-dioxide closed-loop Brayton cycles to achieve high efficiencies with a relatively simple cycle design and compact turbomachinery. To achieve 50% cycle efficiency, high temperatures (≥ 700 °C) and pressures (≥ 20 MPa) are required.

- Projects have been funded to develop new cost-effective and efficient turbomachinery for s$CO_2$ cycles.
- Thermodynamic analyses of alternative s$CO_2$ cycles that can operate with CSP systems are being performed to optimize the design and performance.
- Heat exchangers that can replace the relatively expensive diffusion-bonded heat exchangers currently used have been investigated. Heat exchangers for effective particle/s$CO_2$ heat exchange and s$CO_2$ recuperation are also being sought.

**Air-Brayton Cycles.** Air-Brayton cycles require high temperatures (~1200 °C) for efficient operation. Developing these high temperatures with volumetric air receivers for CSP applications is challenging.

- High-temperature combustors have been examined for CSP hybridization in air-Brayton systems.
- An air-Brayton system employing thermochemical-particle heat collection and storage is being pursued as part of the ELEMENTS program.

**Combined Cycle.** Combined cycles typically employ a high-temperature gas-turbine air-Brayton cycle as the “topping” cycle, and the waste heat from the Brayton cycle is then used to heat steam for a “bottoming” steam-Rankine cycle. Challenges include integrating CSP heating within either the topping or bottoming cycle.

- Systems augmenting natural-gas combined-cycle power plants with solar thermochemical fuels (methane) have been investigated.
- Combined-cycle systems have been proposed that heat the topping gas turbine cycle to ≥ 1100 °C with CSP and augment heating of the bottoming cycle.

**Cooling.** Power cycles require cooling of the working fluid so that the fluid can be efficiently pumped to the heater. Waste heat from the cooling can be significant and new methods are needed to improve the cooling efficiency, which can increase the overall cycle efficiency. In addition, CSP plants operate in desert environments so dry cooling is often required.

- ARPA-E's Advanced Research In Dry cooling (ARID) program has funded a number of projects to improve power-plant cooling.
    - Phase-change materials and heat pipes to transfer heat from power-plant condensers to thermal storage units at night.
    - Enhanced dry-cooling technologies that use boundary-layer disrupting technologies.
    - Desiccant systems to extract water vapor from natural-gas combined-cycle flue gas for use in supplemental evaporative cooling.
    - Low-cost passive radiative cooling structures to more effectively radiate to space.
    - Polymer-composite heat exchangers for radiative cooling of the condenser while preventing evaporation.

### 3.2.5 Soft Costs

In CSP, environmental issues such as glint and glare and avian hazards have raised concerns. Reflected sunlight from collectors in standby mode or while moving to or from off-target positions can cause bright glare to observers such as pilots (Ho et al. 2015). High solar-flux regions at heliostat standby aim points have been shown to cause singeing of birds (McCrary et al., 1986) and some avian mortality has been observed at the latest generation of utility-scale solar plants (PV and CSP) due to collision with structures and solar flux (Walston et al. 2015; Ho, 2015). Costs associated with permitting, monitoring, and operations to address these environmental concerns can be very high; for example, concerns raised at the Ivanpah Solar Electric Generating System have delayed the permitting of the proposed Palen Solar Power Tower CSP plant in Riverside, California.

**Glare.** Concerns regarding glare have been reported at both CSP and PV facilities. Reports of glare from Ivanpah have required new monitoring and operational requirements. New heliostat aiming strategies are required to reduce the glare and solar flux associated with standby positions for power-tower systems. Spreading the heliostats' aim points can reduce the solar flux, but glare can still be prevalent and movement times need to be minimized to the receiver in order to maintain operational performance. Algorithms and aiming strategies are being studied to reduce flux, glare, and movement times.

**Avian Hazards.** Utility-scale solar plants, like all human structures, influence wildlife. Bird mortality has been reported at PV and CSP plants in California, and systematic analysis of the level of fatalities and associated causes are just being developed (Walston et al. 2015; Ho, 2015). Recent full-year data from Ivanpah indicates that total estimated bird deaths were about tenfold lower than some had feared based on preliminary extrapolations (H.T. Harvey & Associates 2015). Although some fatalities are inevitable, changes in heliostat control strategies are being made to limit zones of high flux during standby and minimize the threat from solar flux.

The reported impact to migratory bird mortality was reported as "low." However, it is recommended that the impact of utility-scale solar plants on wildlife continue to be monitored to develop and validate methods to further reduce avian fatalities (H.T. Harvey & Associates 2015).

# 4 Update on CSP System Cost and Performance on the Path to SunShot

## 4.1 Cost and Performance

The performance and cost of CSP plants varies by technology, configuration, solar resource, and financing parameters. A typical methodology used for evaluating different plant designs and technologies within a single index is to derive the levelized cost of electricity. LCOE takes into account the available solar resource, upfront capital investment, plant capacity factor, operations and maintenance (O&M) costs, and financing parameters. LCOE is generally expressed in terms of cents per kilowatt-hour (kWh). Although LCOE does not account for the value of the energy delivered by a given technology (see the following section for more on this topic), it has been chosen as the primary metric used by DOE to track cost reductions targeted by the SunShot program. Alternatively, the capital cost of a CSP plant can be expressed in terms of dollars per watt or, more commonly, dollars per kW. LCOE takes capacity factor and O&M costs into account, but dollars per kW does not. For example, a 100-MW CSP plant can be built with TES and additional collector area to increase its capacity factor. This hypothetical design might generate 100% more energy per year and have a 60% higher installed cost than an alternative design without TES and additional collector area; such a plant would have a higher installed dollars-per-kW cost but a lower LCOE than the alternative plant without TES.

From a technology standpoint, the LCOE of a CSP plant can be reduced in two ways: 1) by lowering capital or O&M costs, and 2) by increasing annual performance. The capital equipment for a CSP plant involves solar components (e.g., solar collector field, heat-transfer piping, and TES system) and conventional thermodynamic power-cycle components (e.g., pumps, steam turbine, generator). The O&M cost per MWh, of which labor cost is the largest contributor, decreases with an increase in plant size or co-location of multiple units at one site. Decreasing capital and operating costs can be achieved by technology advances and increased manufacturing volume and supply-chain efficiency.

The performance of a CSP plant is characterized by its annual solar-to-electric conversion efficiency. This metric includes all of the energy losses that affect the annual electricity produced by the plant, including optical, thermal, and parasitic losses, as well as forced and planned outages for maintenance. Although higher efficiency often entails a higher installed cost, it may more than pay for itself over the operating life of the plant. Also, plants with higher efficiency require less land to produce a given amount of electricity. In other cases, a slightly lower overall efficiency may be advantageous. For example, if the marginal cost of a heliostat is less than the return in revenue it provides, it may be worth adding heliostats, even if it lowers the efficiency of the plant when one normalizes by total reflector area.

While solar-to-electric conversion efficiency measures fundamental technical performance, a more useful metric for power generation is the plant's capacity factor, defined previously as the ratio of actual annual generation to the amount of generation had the plant operated at its nameplate capacity for the entire year. Capacity factors vary greatly between different locations, technologies, and plant configurations; for example, plants with TES achieve higher capacity factors because their power block can have more hours of operation. Capacity factor is used as the metric for tracking power generation per installed unit of capacity, given the different technologies and configurations possible with CSP systems.

## 4.2 CSP Assumptions in the 2012 Vision Study

The estimated cost of CSP technology in the *SunShot Vision Study* (DOE 2012) was based on reported costs for parabolic trough plants built between 2007 and 2010 in Spain and the United States. These costs and future performance and cost objectives were described in two "roadmap" reports that preceded SunShot and were developed by NREL and Sandia National Labs in conjunction with DOE and industry (Kutscher 2010; Kolb 2011). The technologies described in these roadmap reports were the basis for the "Roadmap" costs reported in the *SunShot Vision Study* and reproduced in Table 3. NREL developed performance and cost models for the current and anticipated future CSP designs using the System Advisor Model (SAM) as part of the *SunShot Vision Study*.

**Table 3. CSP Cost Analysis with System Advisor Model version 2010-11-09**

| Case | 2010 Trough | 2015 Trough Roadmap | 2015 Tower Roadmap | 2020 Trough Roadmap | 2020 Tower Roadmap | 2020 SunShot Target |
|---|---|---|---|---|---|---|
| **Design Assumptions** | | | | | | |
| Technology | Oil-HTF Trough | Oil-HTF Trough | Salt Tower | Salt-HTF Trough | Salt Tower | s-$CO_2$ Combined-Cycle Tower |
| Solar Multiple | 1.3 | 2.0 | 1.8 | 2.8 | 2.8 | 2.7 |
| TES (hours) | – | 6 | 6 | 12 | 14 | 14 |
| Plant Capacity (MW, net) | 100 | 250 | 100 | 250 | 150 | 200 |
| Power-Cycle Gross Efficiency | 0.377 | 0.356 | 0.416 | 0.397 | 0.470 | 0.550 |
| Cooling Method | wet | dry | dry | dry | dry | dry |
| **Cost Assumptions** | | | | | | |
| Site Preparation ($/m$^2$) | 20 | 20 | 20 | 20 | 20 | 10 |
| Solar Field ($/m$^2$) | 295 | 245 | 165 | 190 | 120 | 75 |
| Power Plant ($/kW) | 940 | 875 | 1,140 | 875 | 1,050 | 880 |
| HTF System or Tower/Receiver ($/m$^2$ or $/kW$_{th}$) | 90 | 90 | 180 | 50 | 170 | 110 |
| Thermal Storage ($/kWh$_{th}$) | – | 80 | 30 | 25 | 20 | 15 |
| Contingency (%) | 10 | 10 | 10 | 10 | 10 | 10 |
| Indirect (% of Direct Costs + Contingency) | 24.7 | 24.7 | 24.7 | 24.7 | 24.7 | 19.7 |
| O&M ($/kW-yr) | 70 | 60 | 65 | 50 | 50 | 40 |

| Case | 2010 Trough | 2015 Trough Roadmap | 2015 Tower Roadmap | 2020 Trough Roadmap | 2020 Tower Roadmap | 2020 SunShot Target |
|---|---|---|---|---|---|---|
| **Performance and Cost** | | | | | | |
| Capacity Factor (%) | 25.3 | 42.2 | 43.1 | 59.1 | 66.4 | 66.6 |
| Total Installed Cost ($/kW) | 4,500 | 7,870 | 5,940 | 6,530 | 6,430 | 3,770 |
| LCOE (¢/kWh, real) [SunShot financial assumptions] | 20.4 | 19.4 | 14.4 | 11.6 | 9.8 | 6.0 |

Source: *SunShot Vision Study* (DOE 2012)

### Parabolic Trough Assumptions in the 2012 Vision Study

The 2020 Trough Roadmap case was based on a 250-MW molten-salt HTF trough at a field temperature of 500 °C, similar to the configuration being tested by Enel at the 5-MW Archimede demonstration in Sicily. The higher temperature improved power-cycle efficiency and dramatically lowered TES cost. Direct storage of the molten-salt HTF in a thermocline system was assumed, and no adjustment in the performance of the TES system was applied, which assumed improvement in the ability to maintain a sharply stratified thermocline and/or sliding pressure turbine operation with minimal efficiency impacts, as suggested by Kolb (2010). Advanced collector designs, employing novel reflector materials and larger-aperture troughs, accounted for the reduced solar-field cost. Operating experience and manufacturing volume were also assumed to lower O&M and capital costs. The major challenge for this case is successful deployment of salt-HTF systems for troughs.

### Power Tower Assumptions in the 2012 Vision Study

The 2020 Tower Roadmap case was based on a 150-MW molten-salt HTF tower with a supercritical steam power-cycle at 650 °C. A slight power-block cost increase was included based on the current ratio of cost for subcritical-steam to supercritical-steam power blocks for coal plants. Direct storage of the molten-salt HTF in a thermocline system was assumed and, as with troughs, no adjustment in performance of the TES system was applied. System availability increased and O&M cost reductions were due to increased operating experience. Improved heliostat designs, along with manufacturing experience and scale, accounted for the predicted reduction in solar-field cost. The major challenge for this case is scale-down of supercritical steam turbomachinery from the 400-MW or larger scale currently deployed for coal plants to the 150-MW size proposed for CSP, as well as deployment of a salt that is stable up at least 650 °C.

### SunShot Options as Assumed in the 2012 Vision Study

The 2020 SunShot case required more aggressive advances in performance improvements and cost reductions than assumed by the roadmap cases. SunShot-level cost reductions assumed an increase in system efficiency by moving to higher-temperature operation (i.e., maximizing power-cycle efficiency) without sacrificing efficiency elsewhere in the system (i.e., minimizing optical and thermal efficiency losses). Likewise, assumed reduction in the cost of the solar field and development of high-temperature TES compatible with high-efficiency, high-temperature power cycles were critical to further driving down costs.

Reaching the SunShot cost target of 6¢/kWh will require cost and performance improvements to all subsystems within a CSP plant. The primary source of efficiency gains is through developing and implementing advanced power cycles, with the leading candidates for CSP applications being supercritical-$CO_2$ Brayton and air-Brayton power cycles.

Developing and testing new solar-receiver designs and materials will be necessary to accommodate the deployment of advanced, high-temperature power cycles. Air-Brayton systems running at temperatures of 1,000 °C and higher may require volumetric receivers or designs with secondary concentrators. Although $sCO_2$ systems will run at lower temperatures (600 °C–800 °C), receivers that employ $CO_2$ as the HTF will require the testing of compatible materials and designs that accommodate high-pressure $CO_2$ systems. Alternatively, an $sCO_2$ Brayton cycle could be mated with a new high-temperature liquid or solid-particle heat-transfer media; but these materials would necessitate their own receiver design changes. Selective receiver-tube surface coatings that maintain high absorptivity while minimizing emissivity and are stable at high temperatures in air are needed for new receiver designs.

Regardless of the power-cycle design, achieving SunShot targets will also require significant reductions in collector costs while minimizing losses in optical efficiency. For example, it is essential to remove material weight from the solar field while maintaining adequate wind-load rigidity and optical accuracy.

Lastly, as temperatures are increased and new HTFs are deployed, new TES systems will need to advance to maintain the relatively high efficiency and low cost of current CSP TES systems. Supercritical steam and supercritical-$CO_2$ power systems are compatible with thermocline and two-tank storage concepts, but salts with stability and low corrosivity at the proposed higher temperatures may be required. Air-Brayton cycles in particular would benefit from low-cost solid-phase storage media or other novel TES concepts.

## 4.3 Updates to Projected CSP Costs

Since the *SunShot Vision Study* (DOE 2012) was published, four additional large CSP projects have come online in the United States (Table 4): the 250-MW Solana trough plant with TES in Arizona, the 250-MW Genesis trough plant in California, the 250-MW Mojave trough plant in California, and the 377-MW Ivanpah direct-steam power tower in California. A fifth large plant, the 110-MW Crescent Dunes molten-salt power tower with 10 hours of TES, is undergoing commissioning tests. The capacities listed are for net power output. The reported installed costs for the most recent plants are reported in Figure 13 (Bolinger and Seel 2015).

**Table 4. Major CSP Plants Built in the United States in the Past Ten Years (SolarPACES)**

| Plant | Installed Capacity ($MW_{AC}$) | Installed Price ($\$/kW_{AC}$) | Technology | Configuration |
|---|---|---|---|---|
| Nevada Solar One | 68 | 4,480 | Parabolic trough | No TES |
| Martin Next-Gen. Solar Energy Center | 75 | 5,670 | Parabolic trough | Hybrid with natural gas combined-cycle plant |
| Solana | 250 | 6,760 | Parabolic trough | With 6 h TES |
| Genesis | 250 | 5,100 | Parabolic trough | No TES |
| Mojave | 250 | 6,160 | Parabolic trough | No TES |
| Ivanpah | 377 | 6,010 | Power tower | Direct-steam generation, no TES |
| Crescent Dunes | 110 | - | Power tower | Molten salt with 10 h TES |

Price information from Bolinger and Seel 2015

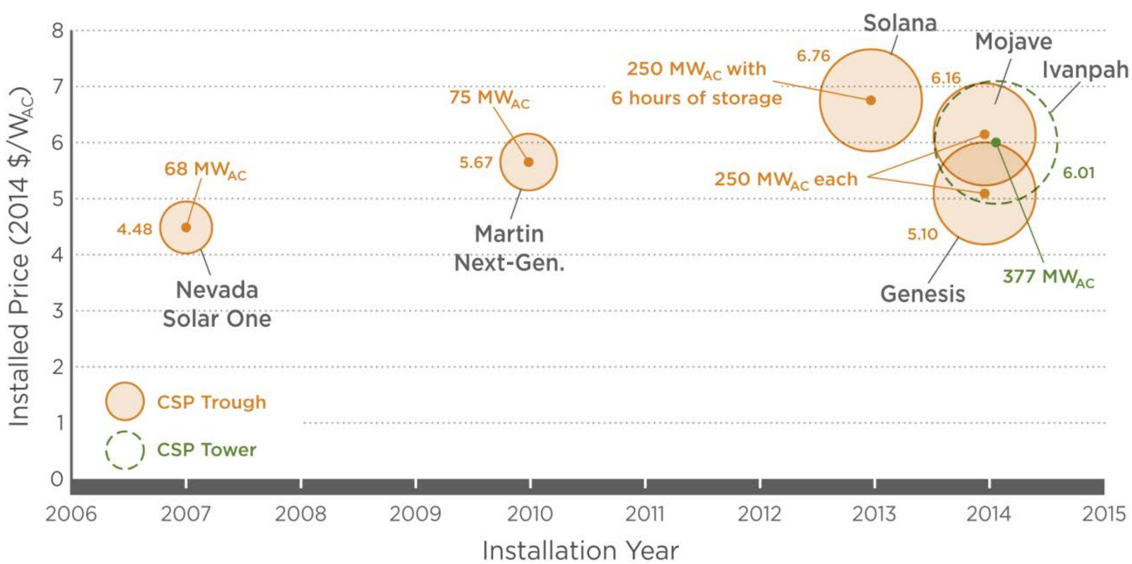


**Figure 13. Historic installed costs for CSP projects in the U.S. from 2007 to 2014**

Source: Bolinger and Seel 2015
Installed price does not account for differences in capacity factor, so comparisons between technologies with and without storage or versus PV installed price are not representative of LCOE differences.

The CSP plants shown in Figure 13 encompass different technologies, systems with and without TES, different cooling systems (which affects cost and efficiency), and different locations (which affects, for example, labor rates and civil/structural requirements). Accordingly, it is difficult to draw conclusions or trends from the limited data. Furthermore, none of the new CSP plant configurations represented in Figure 13 align exactly with the projected costs in Table 3, so it is difficult to assess the accuracy of the earlier projections. In Table 3, 2010 costs are estimated based on a 100-MW parabolic trough plant with no TES (most comparable with the 68-MW Nevada Solar One from 2007), whereas the 2015 costs are based on a 250-MW parabolic trough plant with 6 hours of TES and a 100-MW molten-salt power tower plant with 6 hours of TES. The closest match is a comparison of Solana with the "2015 Trough Roadmap" case. The reported installed cost for Solana is $6,760/kW versus the projected value of $7,870/kW. Important differences include the fact that the Trough Roadmap case assumed a dry-cooled plant whereas Solana is wet-cooled, and the Roadmap used California labor rates versus Solana's construction in Arizona. These two effects would tend to reduce the cost of Solana versus the roadmap assumptions.

NREL has updated its current cost models twice since the publication of the *SunShot Vision Study* (DOE 2012). Early in 2013, NREL published an update for the estimated cost of a molten-salt power tower (Turchi and Heath 2013) and later that year updated the estimated cost of the solar field by modeling BrightSource Energy's LH-2.2 heliostat. This design is used at the Ivanpah plant in southern California and represents a modern, high-production-volume design. About 173,000 heliostats are installed at the three-tower site (Figure 14). The LH-2.2 design uses two glass panels, each 230 cm x 330 cm, for a total reflector area of 15.2 $m^2$. The unit is constructed primarily of steel and glass. NREL estimated the weight of the heliostat, including the mounting pylon, based on published information related to the structural design and inclusion of a representative two-axis drive system. The LH-2.2 heliostat pylons are physically driven into the ground and do not use concrete foundations. NREL's estimated cost for the installed LH-2.2 solar field was $168/m^2$ in 2013$, which is adjusted to $163/m^2$ in 2010$ (and $170/m^2$ in 2015$) using the Chemical Engineering Plant Cost Index (CEPCI); also see Figure 15.

**Figure 14. LH-2.2 heliostats at Ivanpah**

Photo by Gilles Mingasson/Getty Images for Bechtel

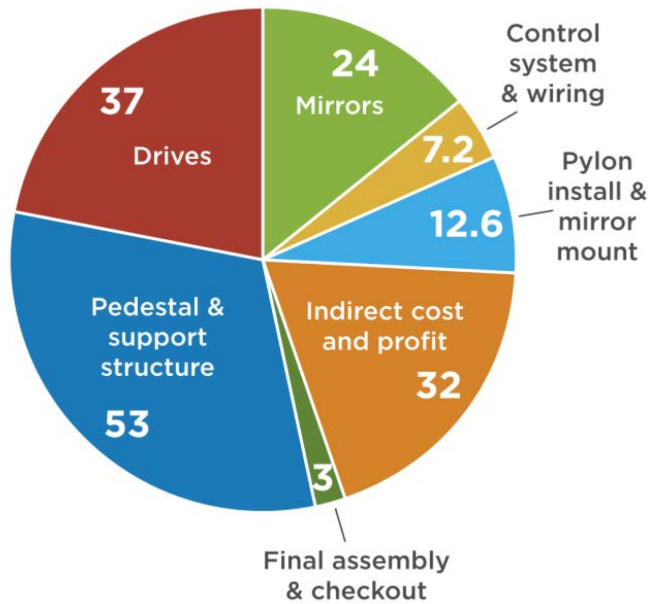


**Figure 15. Cost breakout ($/m$^2$) for the LH-2.2 heliostat used to update NREL's molten-salt power-tower model**

The estimated installed cost was $168/m$^2$ in 2013$.

In 2015, NREL undertook a similar bottom-up cost estimate for two parabolic trough collectors: SkyFuel's SkyTrough and Flabeg's Ultimate Trough (see Table 5). The SkyTrough was eventually selected as the new baseline trough within SAM, with an estimated installed cost of $170/m$^2$. The estimated cost difference between the two designs was very small; however, the SkyTrough was chosen based on greater confidence in the NREL analysis results and more information regarding the unit's performance.

**Table 5. Commercial Parabolic Troughs Examined by NREL's Update to the Current Parabolic Trough Collector Cost**

| Property | SkyTrough | Ultimate Trough |
|---|---|---|
| Manufacturer | SkyFuel (USA) | Flabeg (Germany) |
| Reflector type | Reflectech polymer film | 4-mm glass |
| Aperture width (m) | 6.0 | 7.51 |
| Module length (m) | 13.9 | 24.5 |
| Solar collector assembly (SCA) length (m) | 115 | 247 |
| Modules per SCA | 8 | 10 |
| SCA aperture area (m$^2$) | 656 | 1,689 |
| Frame design | Aluminum spaceframe | Steel torque box |

Source: Kurup and Turchi 2015

## 4.4 Updated LCOE Estimates for the Current Molten-Salt Power Tower and Parabolic Trough Systems

NREL updated the CSP technology cases for 2015 based on cost updates to parabolic trough and power tower solar fields, as well as inflation indexing of more conventional subsystems. In addition to the technology and inflation updates, the SAM model itself changed since 2012 and simulation results vary somewhat due to modifications in the code. The discussion below focuses on projections for the power tower technology, which is viewed as the leading candidate to hit the CSP SunShot targets. Information on updated costs for parabolic trough systems can be found in Kurup and Turchi (2015).Table 6 shows the original 2015 Roadmap case for the molten-salt power tower (see Table 3), but run in SAM-2015-06-30. Changes in SAM's performance and financial models result in slightly different installed cost and LCOE. (Note that SAM 2015 has adopted the term "levelized power purchase agreement" (LPPA) for what was formerly called LCOE in SAM 2010.)

**Table 6. New Cost Projections Based on Use of SAM Version 2015-06-09, Revised Technology Costs for 2015, and Updated Financial Assumptions as Noted**

| Case | 2015 Projection from Tower Roadmap | 2015 Tower with SVS 2012 Financials | 2015 Tower with OTPSS Financials | 2017 Tower | 2020 SunShot Tower |
|---|---|---|---|---|---|
| Source of Technology Cost Assumptions | 2012[a] | 2015[b] | 2015[b] | 2015[b] + this study | SunShot |
| Source of Financial Assumptions | 2012[a] | 2012[a] | 2015[c] | 2015[c] | 2015[c] |
| Technology | Molten-Salt Tower | Molten-Salt Tower | Molten-Salt Tower | Molten-Salt Tower | SunShot 2020 |
| Solar Multiple | 1.8 | 2.4 | 2.4 | 2.4 | 2.7 |
| TES (hours) | 6 | 10 | 10 | 10 | 14 |
| Plant Capacity (MW, net) | 100 | 100 | 100 | 100 | 100 |
| Power-Cycle Gross Efficiency | 0.416 | 0.412 | 0.412 | 0.412 | 0.55 |
| Cooling Method | dry | dry | dry | dry | dry |
| **Cost Assumptions** | | | | | |
| Cost Year | 2010 | 2015 | 2015 | 2015 | 2015 |
| Site Preparation ($/m$^2$) | 20 | 16 | 16 | 16 | 10 |
| Solar Field ($/m$^2$) | 165 | 170 | 170 | 93 | 75 |
| Power Plant + BOP ($/kW) | 1,140 | 1,530 | 1,530 | 1,530 | 900 |
| Tower/Receiver ($/kW$_{th}$) | 180 | 180 | 180 | 180 | 150 |
| Thermal Storage ($/kWh$_{th}$) | 30 | 26 | 26 | 26 | 15 |
| Contingency (%) | 10 | 10 | 10 | 10 | 10 |

| Case | 2015 Projection from Tower Roadmap | 2015 Tower with SVS 2012 Financials | 2015 Tower with OTPSS Financials | 2017 Tower | 2020 SunShot Tower |
|---|---|---|---|---|---|
| Indirect (% of Direct Costs + Contingency) | 17.6 | 17.6 | 17.6 | 17.6 | 13.0 |
| Cost during Construction (% of Overnight Cost) | 6 | 6 | SAM formula | SAM formula | SAM formula |
| O&M ($/kW-yr) | 65 | 66 | 66 | 66 | 40 |
| **Performance and Cost** | | | | | |
| Capacity Factor (%) | 45.2 | 61.3 | 61.3 | 61.3 | 69.1 |
| Overnight Installed Cost ($/kW) | 5,420 | 7,630 | 7,630 | 6,380 | 4,020 |
| Total Installed Cost ($/kW) | 5,750 | 8,090 | 8,160 | 6,820 | 4,300 |
| Levelized Power Purchase Agreement (¢/kWh, real, no ITC) | 14.2 | 14.2 | 12.0 | 10.3 | 5.9 |

[a] *SunShot Vision Study* (DOE2012)
[b] Kurup and Turchi 2015
[c] On the Path to SunShot financials (OTPSS)

Financial parameters for this new analysis were adjusted from those used in the *SunShot Vision Study* (DOE 2012). The original study chose financing assumptions to align with a long-term notion of how these assets might be funded in the future, having a debt-to-asset ratio of 60%, and equity and debt priced similarly to investor-owned utilities and independent power producers. Based on these assumptions, a nominal weighted average cost of capital (WACC) of 8.6% was calculated (5.5% real). For this new analysis, we incorporate some of the financial progress that has been made since the original study and provide more current assumptions for the cost of financing. We assumed that the project is funded through tax and sponsor equity, with both providing 50% of the capital. Further, the sponsor uses back-leverage mezzanine debt to fund the majority of its capital, although it is limited by a debt-coverage ratio of 1.4. Through these parameters, a nominal WACC of 7% was calculated (4.4% real).

In Table 6, two current 2015 cases are shown using the former and OTPSS financial assumptions. These cases are based on the solar-system cost updates undertaken in 2013 and 2015 (Kurup and Turchi 2015). The heliostat solar field cost is estimated at $\$170/m^2$ in 2015, which is very close to the estimate for 2015 made in the 2012 Vision Study. The SunShot case is shown with the new financial assumptions. In addition to the cases presented in Table 5, a near-term scenario is evaluated that assumes rapid deployment of one or more heliostat designs that are currently in the research and development stage. An assessment of these designs suggests that installed cost in the range of $\$93/m^2$ is possible when the system(s) reach the marketplace (Stekli 2015). To evaluate the effect of this potential, the 2015 case in Table 6 is repeated with the solar-field cost adjusted from $\$170/m^2$ to $\$93/m^2$. The results of this scenario (labeled as "2017 Tower") and other cases from Table 6 are shown in Figure 16, which highlights the contribution to LCOE for a progression of the cost categories in Table 6.

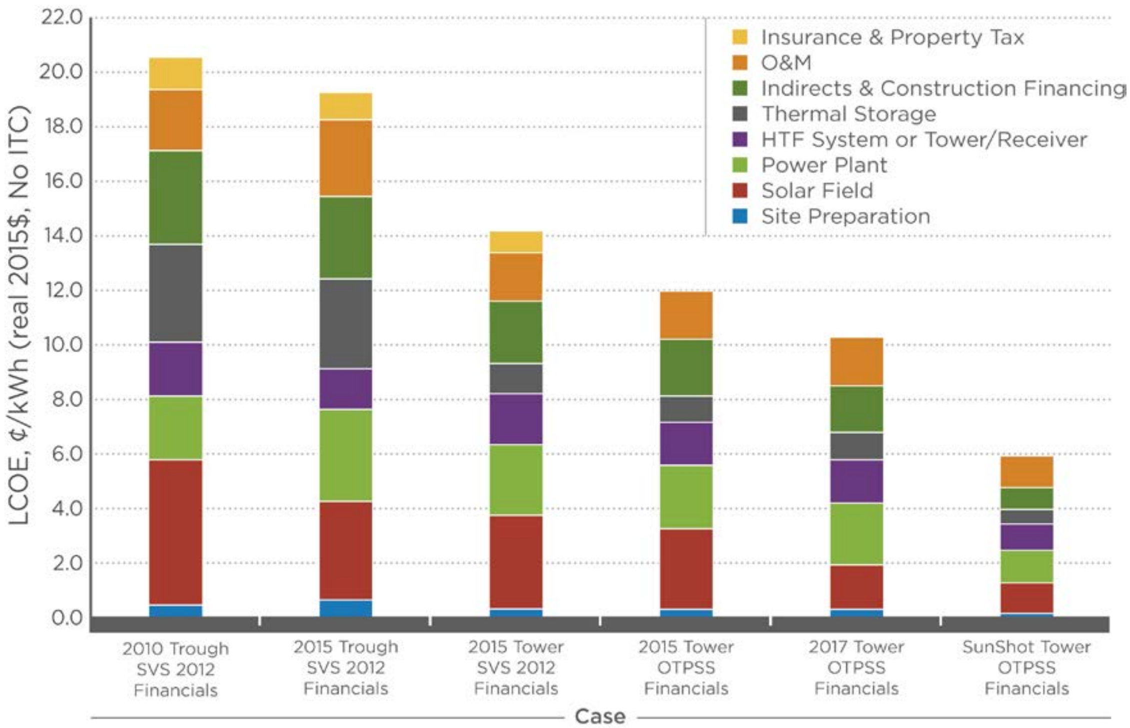


**Figure 16. Cost category contributions to LCOE for the cases shown in Table 6**

In addition to the updated estimates for solar-field costs, other subsystem costs have been adjusted to 2015 dollars by indexing with the CEPCI. The CEPCI includes a composite index and ten individual indices representing cost categories such as “heat exchangers & tanks” and “construction labor.” NREL’s plant models use CEPCI indices that are most suited for each cost category (e.g., the “heat exchangers & tank” index is used to adjust the steam-generation system) as described in the spreadsheet-based plant models for the parabolic trough and molten-salt power tower (see SAM website at sam.nrel.gov/cost).

In comparing the estimated capital costs from the *SunShot Vision Study* (DOE 2012) and the current analysis, we find that the predicted 2015 decline in heliostat cost was fairly accurate. However, some of the advantages of these lower costs have been offset by inflationary increases for more conventional subsystems such as tanks, heat exchangers, and turbomachinery. Prices for salt and oil influence the cost of the HTF and thermal storage systems, with the price for oil HTF being particularly volatile.

# 5 Assessment of CSP SunShot Targets for Non-Baseload Applications

## 5.1 Net System Cost and Application to SunShot

Considerable literature has covered the economic analysis of CSP-TES systems, with an emphasis on determining the LCOE as described in the previous section. The LCOE is generally emphasized when assessing the economic viability of renewable energy systems. However, LCOE does not reflect the operational and capacity value of CSP, which varies substantially for configurations ranging from low-capacity-factor peaking plants to high-capacity-factor baseload systems—the latter being the configuration identified to achieve the SunShot target. CSP-TES can be dispatched in a similar manner to conventional thermal generation, so the emphasis on LCOE alone is an incomplete economic assessment when compared against variable-generation renewable technologies such as PV or wind.

A more comprehensive methodology—an assessment of the net system cost—includes comparisons of both the costs and grid-wide system benefits of different technologies. The net system cost (or alternatively, net cost) of a resource represents the difference between the annualized costs of adding a new conventional or renewable generating technology (e.g., CSP-TES, PV, combustion turbines, combined cycle) and the avoided cost realized by displacing other resources providing the same level of energy and reliability to the system (Mills and Wiser 2012). For variable-generation wind and solar resources, the total avoided cost is dominated by avoided operational costs, which are primarily avoided fuel and emissions. On the other hand, the dispatchable nature of CSP-TES allows the technology to optimally displace more expensive generation (e.g., generation from inefficient combustion turbines or lower-performing combined-cycle or steam plants), while simultaneously providing firm capacity. As described in several NREL reports (e.g., Madaeni et al. 2011; Denholm et al. 2013; Jorgenson et al. 2014), the ability of CSP-TES to provide firm capacity greatly enhances its economic value relative to variable-energy resources. The following section provides an overview of the tools and methodologies used to arrive at the net system benefit for CSP-TES relative to other generation resources.

## 5.2 Overview of Tools and Methodology

### *5.2.1 Determining the System Benefit*

The overall system benefit is derived from the operational and capacity benefits provided by a generator supplying energy to the grid. For this and similar analyses, NREL has evaluated the operational value of conventional and renewable energy technologies using PLEXOS, a commercially available production-cost modeling software, to simulate the power grid in California. Production cost modeling software allows grid planners and operators to assess many aspects of power generation, including system costs and emissions. The database used for this analysis contains generator-level details of California's electricity sector as well the rest of the Western Interconnection. Production cost models such as PLEXOS are formulated to minimize the total cost of generating electricity to serve energy demand at every time step by *committing* (i.e., determining whether a generator is on or off) and *dispatching* (i.e., adjusting the output of the committed generators). A detailed description of the methodology is described in Denholm and Hummon (2012).

In this update, we assessed a midterm trajectory for California with 40% renewable energy penetration, about half of which is derived from solar PV, and then considered the economic impacts of incremental additions of CSP-TES and conventional generation to an existing generation portfolio. A 40% scenario for California was chosen because the state represents a significant market for CSP. This is due in part to the quality of the resource and California's goal of achieving 50% of non-distributed energy generation from renewables by 2030 (Richardson 2015). Achieving this goal will likely result in significant penetration of variable resources and will perhaps increase the need for energy storage.

The modeling approach assumes that retirements of older generation capacity will necessitate an increase in firm generator capacity. 1,500 MW of retired capacity was assumed in order to generate quantifiable operational benefits when replacing that generation with new capacity. The increase in firm generator capacity can come from high-efficiency gas combustion turbines (CTs), combined-cycle gas plants (CCs), or CSP-TES. For this analysis, we assumed that all CSP configurations include a minimum of 6 hours of TES to maintain firm capacity, as described previously in Table 1. We assumed that conventional generators (gas CTs and CCs) earn a full capacity credit of the same magnitude as those earned by configurations of CSP-TES.

### 5.2.2 Determining the Operational Value of Incremental Additions

With any incremental addition of generation capacity, PLEXOS accounts for all sources of generation that the new asset displaces based on minimizing the overall operational cost of the system. For CSP-TES, the marginal cost of energy produced is very low due to the lack of fuel and emissions costs, which comprise the vast majority of operating expenses for power plants in this system. For the conventional generators, we assumed either the addition of new high-efficiency gas CT or CC plants. Because CTs provide energy with relatively high marginal cost, they have low capacity factors but may still displace some energy from even more costly generators. The CC plant operates at lower heat rate and therefore operates at relatively higher capacity factors. Heat-rate assumptions and resulting capacity factors returned from PLEXOS are shown in Table 7.

**Table 7. Performance Assumptions and Capacity Factors for Conventional Generators**

| Assumptions for Modeling Generator Performance | | |
|---|---|---|
| Generator Type | Heat Rate (Btu/kWh)[a] | Capacity Factor (%)b |
| Combustion Turbine | 9,500 | 12.0 |
| Combined Cycle | 7,500 | 43.3 |

[a] A single heat rate was used for CT due to operation at full load whereas a multi-point heat rate was used to model the CC based on regular operation at part load.
[b] Based on PLEXOS results

The incremental avoided operation costs were evaluated by simulating one operating year for the power system of the western U.S., including California. Table 8 shows the key assumptions regarding system costs. For a detailed discussion of all model inputs, see Brinkman (2015).

**Table 8. Modeling Assumptions Impacting System Operational Costs**

| | Modeling Assumptions for Operational Analysis |
|---|---|
| Dollar Year | 2014 |
| Simulation Year | 2025 |
| Natural Gas Price (low/high) | \$3.5–\$6.1 / MMBtu |
| Carbon Emissions Cost (low/high) | \$13–\$32.4 / metric ton |

A subset of the SM/TES combinations of technologies, shown in Table 1, was included in the production cost model to replace the assumed 1,500 MW of retired fossil-fired steam turbines. The annual avoided costs are the difference between a run with and without the additional technologies. The value of avoided energy is largely determined by the assumed natural gas price, because gas generators are typically the marginal resources displaced by added renewables. The annual avoided costs also include any reduction in carbon costs, as well as reduced variable operations and maintenance (VO&M) and start costs from the conventional generator fleet. We assumed low and high values for natural gas price and emissions cost to assess the sensitivity of operations savings to these two variables. The Results section details the avoided costs for each scenario shown in Table 9.

**Table 9. Modeling Scenarios**

| Technology | Capacity (MW) | Energy (GWh annual) | Capacity Factor (%) |
|---|---|---|---|
| Combustion Turbine | 1,500 | 1,580 (3,350) | 12.0 (25.5)[a] |
| Combined Cycle | 1,500 | 5,690 (11,270) | 43.9 (85.8) |
| CSP-TES (peaker, SM = 1, 6 h TES) | 1,500 | 3,220 (3,230) | 24.5 (24.6) |
| CSP-TES (intermediate, SM = 2, 9 h TES) | 1,500 | 6,300 (6,300) | 47.9 (47.9) |
| CSP-TES (baseload, SM = 3, 15 h TES) | 1,500 | 8,910 (9,240) | 67.8 (70.3) |

[a] Values in parentheses are results for the high natural gas and emission cost scenario.

### 5.2.3 Determining the Upfront Capital Costs of Incremental Additions

The net system cost is determined by subtracting the annualized system savings described in the previous section from the capital and fixed O&M costs of the new generator. Current and future CSP-TES costs were estimated for each CSP configuration described in Table 9.

The costs for CSP were annualized based on a simple calculation for fixed charge rate using the equation

$$\text{Total Annualized Cost} = \text{FCR} \times C_C + \text{FOM}$$

where FCR is the fixed charge rate, $C_C$ is the installed capital cost including construction financing, and FOM is the annualized fixed O&M cost levelized to account for escalation. A description of each of these factors and their associated equations is provided in the SAM help guide (SAM version 2015-06-30).

### 5.2.4 Determining Annualized Costs for CSP-TES

We used SAM (version 2015-06-30) to generate the upfront capital costs for each CSP-TES configuration. Upfront costs include overnight capital in addition to construction finance costs. We used the SAM "Generic Model" to estimate CSP-TES tower capital cost and performance based on the current molten-salt tower and SunShot tower configurations described in Section 4. The generic model allows for increased flexibility and speed when estimating the cost and performance of future CSP-TES systems integrated with advanced power cycles anticipated to operate at higher temperatures than today's Rankine-based systems. The SAM molten-salt power tower (MSPT) model allows for separate designations of heliostat and receiver costs; however, the generic model requires that both costs be folded together into a single value in terms of dollars per square meter of solar field. Cost and performance assumptions used to generate upfront capital and O&M costs are given in Table 10.

**Table 10. Assumptions for Current and Future CSP-TES Tower Scenarios**

| Case | CSP-TES Tower (current) | CSP-TES Tower (SunShot) |
|---|---|---|
| Location | Daggett, CA | Daggett, CA |
| System Costs | | |
| - Site improvements ($/m$^2$) | 10 | 10 |
| - Solar field (heliostat and receiver)[a] ($/m$^2$) | 260 | 160 |
| - Thermal energy storage ($/kWh$_t$) | 27 | 15 |
| - Power block ($/kW$_e$) | 1,550 | 880 |
| - EPC and owners costs | 10% of direct costs | 10% of direct costs |
| - Land costs ($/acre) | 10,000 | 10,000 |
| - Fixed O&M ($/kW-yr) | 65 | 40 |
| - O&M escalation (%) | 2.5 | 2.5 |
| Construction loan period and interest rate | 24 months at 6% | 24 months at 6% |
| Cycle Performance | | |
| - Cycle gross efficiency (%) | 41.2 | 55 |

[a] Value changes slightly with solar multiple based on conversion of $150/kWh$_t$ receiver cost to $/m$^2$

### 5.2.5 Determining Annualized Costs for Combustion Turbine and Combined-Cycle Plants

The California Cost of Generation model (COG model version 3.98) was used to estimate the capital cost of a new CT or CC plant. The COG model is a spreadsheet model that calculates cost for electric generating technologies. The COG model generates average, low, and high estimates for levelized and total annualized capital costs for both generating technologies. For this report, we used the model to estimate the average cost for California for new merchant 200-MW aeroderivative combustion turbine and 500-MW duct-fired combined-cycle plants. The annualized costs for each generator are summarized in Table 11.

**Table 11. Assumptions for New Combustion Turbine and Combined-Cycle Plants**

| Generator Type | $/kW-yr |
|---|---|
| **Combustion Turbine** | |
| - Capital and Financing – Construction | 115.48 |
| - Insurance | 7.90 |
| - Ad Valorem Costs | 11.50 |
| - Fixed O&M | 33.08 |
| - Corporate Taxes | 33.35 |
| ***Total Fixed Costs (Combustion Turbine)*** | ***201.31*** |
| | |
| **Combined Cycle** | |
| - Capital and Financing – Construction | 117.66 |
| - Insurance | 7.91 |
| - Ad Valorem Costs | 11.52 |
| - Fixed O&M | 45.31 |
| - Corporate Taxes | 38.81 |
| ***Total Fixed Costs (Combined Cycle)*** | ***221.21*** |

Financial parameters used in the COG model are shown in Table 12. The resulting fixed charge rate was similarly used to calculate the annualized cost for each CSP-TES configuration, allowing for an equal comparison between each technology option.

**Table 12. COG Model Financial Parameters**

| Financial Parameter | Value |
|---|---|
| Federal Tax Rate (%) | 35.0 |
| State Tax Rate (%) | 8.84 |
| Equity Internal Rate of Return (%) | 13.25 |
| Debt Rate (%) | 4.52 |
| Debt Term (years) | 10 |
| Debt (%) | 67 |
| Economic Life (years) | 30 |
| Inflation Rate (%) | 1.52 |
| **Calculated FCR (%)** | **7.01** |

## 5.3 Results

As discussed in Sec. 5.1, the total system cost is calculated by subtracting the annual operational value from the sum of the upfront capital and fixed costs. The net cost was calculated for each of the technologies and configurations shown in Table 9.

### *5.3.1 Annualized Net System Cost for Low Natural Gas and Carbon Price Scenarios*

Table 13 and Figure 17 show the full results for the low natural gas price and emission cost scenario that is representative of current market conditions in California (see Table 8). Table 13 shows the annual system benefit for each scenario, as well as the annualized capital cost under current costs and under SunShot cost targets for CSP. The first-year cost subtracts the annualized value from the capital cost. The total net system cost is also shown in Figure 17 for each cost trajectory.

**Table 13. Annualized Operational Value, Capital and Fixed Costs, and Net Cost for Each Scenario, Using the Low Natural Gas and Emissions Cost Assumptions**

| Scenario | Annualized Operational Value ($M) | Annualized Cost Under Current Scenario ($M) | Annualized Cost Under SunShot Scenarios ($M) | Net Annualized Cost for Current Scenarios ($M) | Net Annualized Cost for SunShot Scenarios ($M) |
|---|---|---|---|---|---|
| Combustion Turbine | 15 | 301 | 301 | 286 | 286 |
| Combined Cycle | 26 | 331 | 331 | 305 | 305 |
| CSP-TES (peaker, SM = 1, 6 h TES) | 117 | 675 | 362 | 557 | 245 |
| CSP-TES (intermediate, SM = 2, 9 h TES) | 211 | 947 | 485 | 736 | 274 |
| CSP-TES (baseload, SM = 3, 15 h TES) | 295 | 1,274 | 633 | 980 | 338 |

Figure 17 shows the current and SunShot CSP results compared against conventional CT and CC. Note that for current CSP costs, peaking configurations provide the lowest net system cost, although costs are still roughly double those for conventional generation. However, for the SunShot scenarios, both peaking-load and intermediate-load CSP compare favorably against the conventional generators. The values provided alongside each bar in the figure represent LCOEs calculated using SAM. A comparison of the net system costs vs LCOEs provided in the figure demonstrates the value of using the net system cost as an alternative metric to LCOE. Using the SunShot scenarios as an example, the LCOE for each CSP configuration is lower for the baseload system in comparison to the peaking or intermediate load. However, the net system cost is highest for the baseload system compared to the other CSP configurations. Based on this scenario, a utility would choose the peaking CSP plant relative to the alternative technology options, including the conventional natural-gas-fired generators.

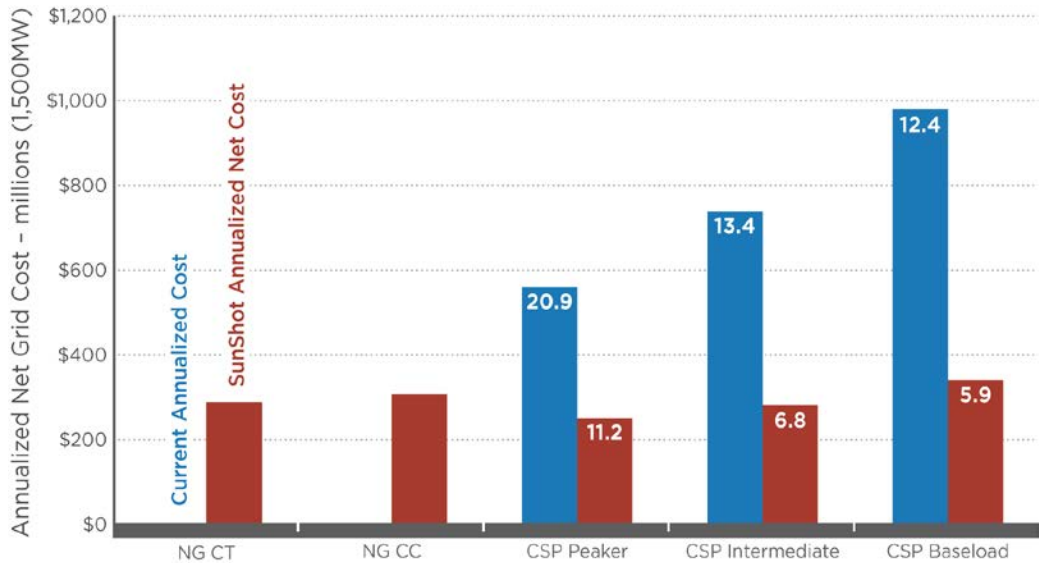


**Figure 17. Comparison of annualized net cost of current and SunShot CSP configurations (peaker, intermediate, baseload) and conventional combustion turbine and combined-cycle plants assuming low natural gas and emission cost scenarios**

Values shown are LCOEs calculated by SAM for each CSP configuration.

### *5.3.2 Annualized Net System Cost for High Natural Gas and Carbon Price Scenarios*

Table 14 shows the full results for the high natural gas price and emission cost scenarios described in Table 8. The change in natural gas and emission costs influences both the dispatch order for the conventional generators (see capacity factors provided in Table 9) as well as the avoided cost of fuel and emissions.

**Table 14. Annualized Operational Value, Capital and Fixed Costs, and Net Cost for Each scenario, Using High Natural Gas and Emissions Cost Assumptions**

| Scenario | Annualized Operational Value ($M) | Annualized Cost Under Current Scenario ($M) | Annualized Cost Under SunShot Scenarios ($M) | Net Annualized Cost for Current Scenarios ($M) | Net Annualized Cost for SunShot Scenarios ($M) |
|---|---|---|---|---|---|
| Combustion Turbine | 9 | 301 | 301 | 292 | 292 |
| Combined Cycle | 31 | 331 | 331 | 301 | 301 |
| CSP-TES (peaker, SM = 1, 6 h TES) | 152 | 675 | 363 | 523 | 211 |
| CSP-TES (intermediate, SM = 2, 9 h TES) | 305 | 947 | 485 | 642 | 180 |
| CSP-TES (baseload, SM = 3, 15 h TES) | 453 | 1,274 | 633 | 822 | 180 |

Figures 18A and 18B provide a closer look at CSP configurations in the SunShot case, including both the low and high natural gas/emission cost scenarios. Uncertainty bands shown in the figures assume a ±10% variation in each of the most influential model parameters (see Figure 19).

Clearly, there is a preference toward choosing the peaking configuration for the low natural gas and emission cost scenarios. However, this decision becomes less clear when viewing the results for the high natural gas and emission cost scenarios—where, when considering uncertainty, each of the CSP configurations compares similarly against the conventional alternatives.

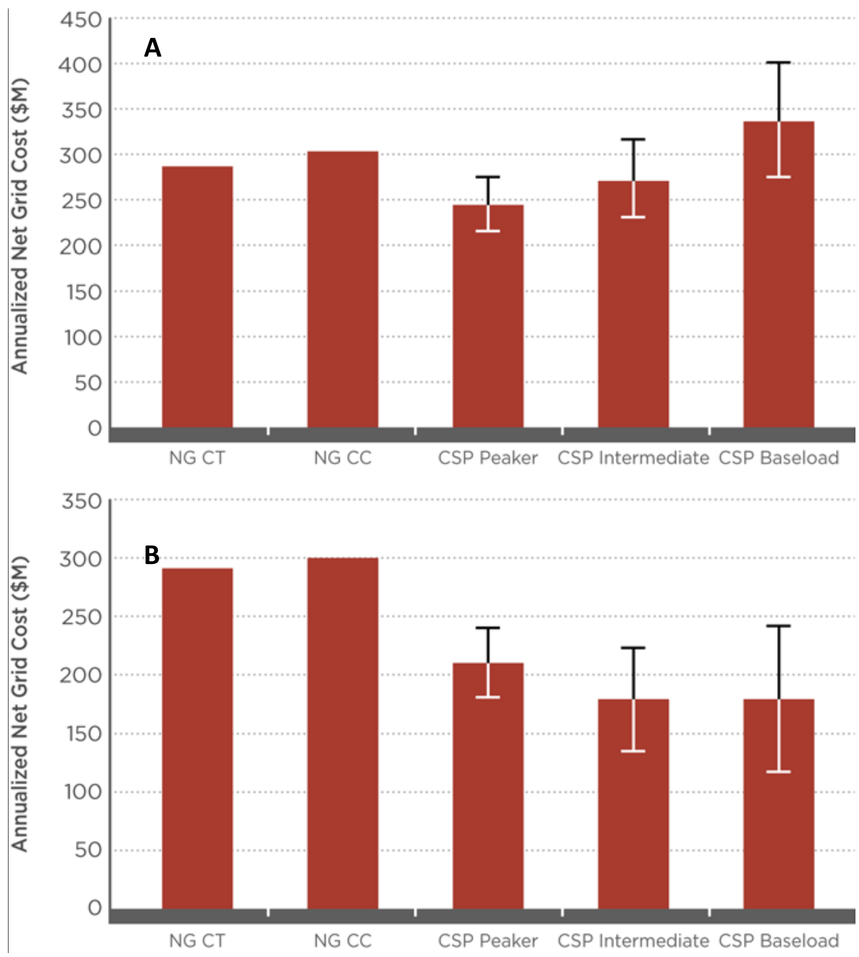


**Figures 18. Low natural gas and emission cost scenario (A) and high natural gas and emissions cost scenario (B)**

Comparison of net cost for SunShot CSP configurations;
Uncertainty bars represent ±10% variation in SunShot parameters.

Finally, the sensitivity of each of the key SunShot parameters that influence the LCOE and total system cost was determined. Figure 19 shows the standardized rank-order coefficient based on a stepwise rank regression analysis of the 500 model runs used to determine the uncertainty bands for each of the configurations shown in Figures 18A and 18B.

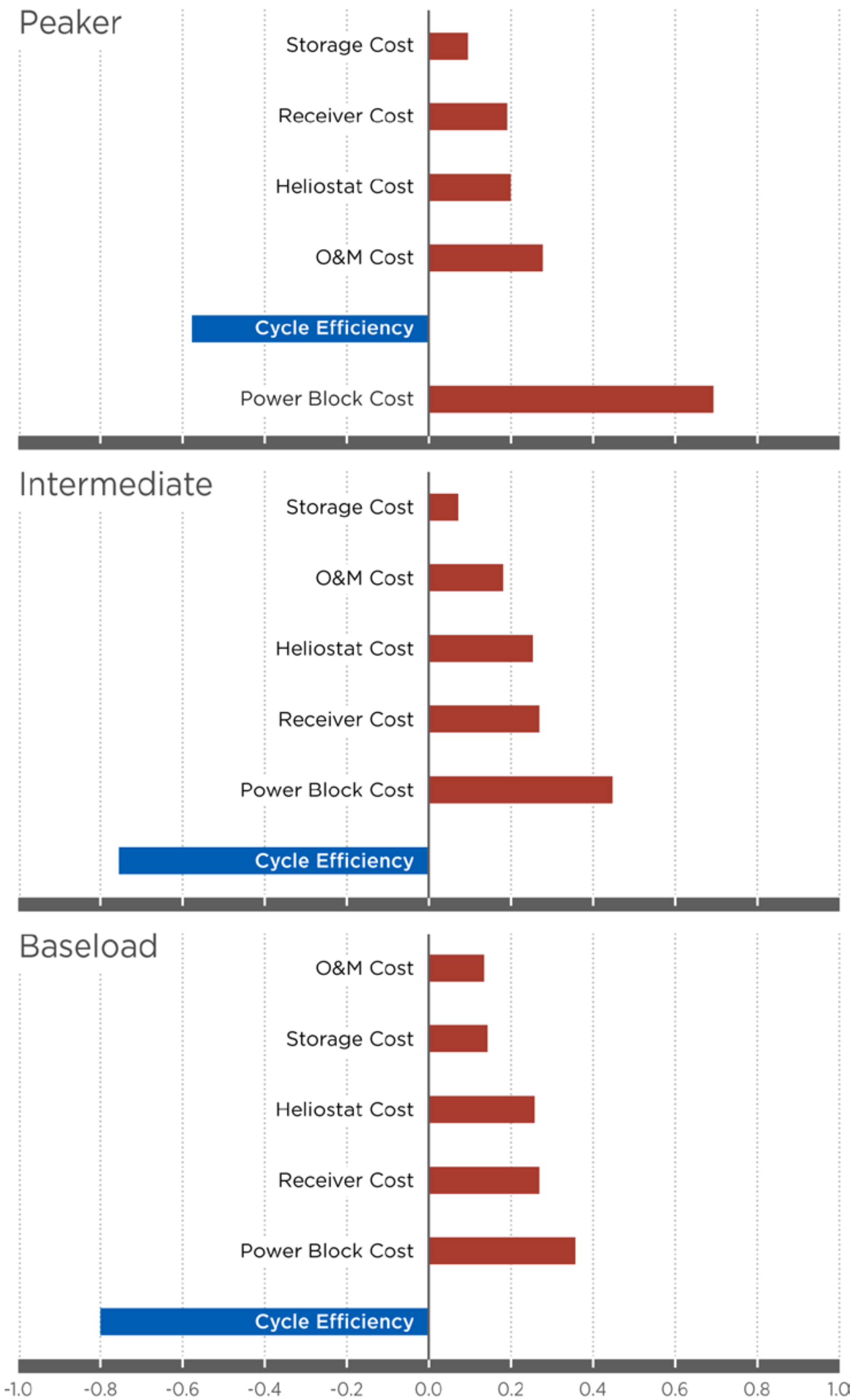


**Figure 19. Standardized rank-order coefficients for peaker, intermediate, and baseload CSP configurations**

Figure 19 demonstrates the change in sensitivity to each of the SunShot parameters for each of the CSP-TES configurations considered in this analysis. Although it is clear that cycle performance is important for each of the systems considered, the cost of the power block plays a dominant role when considering peaker configurations. O&M costs for peaking configurations are also a more important consideration relative to the systems having higher capacity factor. For all configurations, the solar-field costs including both the heliostat and receiver are important, but have a lesser influence on the overall system cost once the SunShot targets have been realized. Storage costs have the smallest influence for all configurations studied.

### 5.3.3 Comparison of Net Benefit of CSP-TES with PV and Batteries

The methodology discussed above that compares the net benefit of CSP-TES to conventional fossil-fueled generation can also be applied to comparisons between CSP-TES and solar PV. In this section, we summarize work that compared the annualized costs of CSP-TES, PV with batteries, and PV with CTs, each providing reliable capacity under an assumed scenario of 40% renewable penetration within the state of California (Jorgenson et al. 2015).

As stated previously, the state of California represents an important market due to its legislation to increase renewable energy deployment and its impressive solar resource. The cost of solar PV has dropped rapidly recently, making it an attractive option for procuring renewable energy toward the state's 50% RPS. Although CSP-TES has yet to experience the same cost decline, CSP-TES has an inherent advantage over PV due to its dispatchability, that is, its ability to shift energy in time. This ability establishes two distinct advantages for CSP-TES. First, dispatchability allows CSP-TES to shift its energy in time as discussed in Section 5.2. Second, CSP-TES can provide firm capacity, which is generation capacity available to the power system at times of greatest need, including hours of the highest net demand. Solar PV alone cannot provide either of these two benefits, but could be deployed with other technologies that are able to do so, such as battery storage or conventional gas turbines.

In this analysis, we similarly analyzed a situation in which California retires old generation assets and must procure 1,500 MW of firm capacity; in addition, California must procure renewable energy to progress toward the mandated RPS. CSP-TES can provide both firm capacity and renewable energy. Solar PV can provide renewable energy and some firm capacity,[1] but deployments of PV must be coupled with other sources of firm capacity. This results in the following options for procurement:

1. CSP-TES, with various configurations
2. Solar PV with long-duration lithium-ion battery
3. Solar PV with conventional gas combustion turbine

[1] In this analysis, PV receives a capacity credit of 20%, meaning that 20% of its rated capacity is considered "firm." Significant deployment of PV considered here would likely reduce the capacity credit further, but we adopt the 20% value for a conservative comparison to CSP-TES. For more details, see Jorgenson et al. 2015.

These options can be compared with their net costs, or their total costs minus total benefits. In this case, costs include annualized upfront capital costs with fixed costs. Table 15 shows a simplified version of these costs. Benefits represent the operational value of each option as discussed in Section 5.1 (see Jorgenson et al. 2015 for a more detailed breakdown of costs and benefits for each technology option).

**Table 15. Capital Costs for all Options**

| | Current Costs | | Future Costs | |
|---|---|---|---|---|
| **Technology** | **Initial Costs ($/kW)** | **Annual Costs ($/kW-yr)[a]** | **Initial Costs ($/kW)** | **Annual Costs ($/kW-yr)** |
| Combustion Turbine | – | 190 | – | 190 |
| Battery (Li-ion, 6-h duration) | 3,000–6,000 | *5–10-yr replacement* | 1,100–2,200 | *10–15-yr replacement* |
| Solar PV | 1,910 | 17 | 1,050 | 12 |
| CSP-TES (various configurations) | 4,410–10,500 | 73 | 2,210–4,870 | 40 |

[a] Annual cost for gas CT includes capital cost, financing, insurance, taxes.

The first-year cost then subtracts the annual operational value from the annualized sum of the upfront capital and fixed cost. The analysis includes two cost scenarios: current costs and future costs. The future costs represent both CSP-TES and PV reaching the SunShot cost targets.[2] The results are shown in Figure 20. For the case of PV with batteries, error bars represent the range of battery costs and replacement periods indicated in Table 15.

[2] SunShot does not include cost projections or targets for batteries. Instead, the projected battery costs are based on referenced sources for future costs.

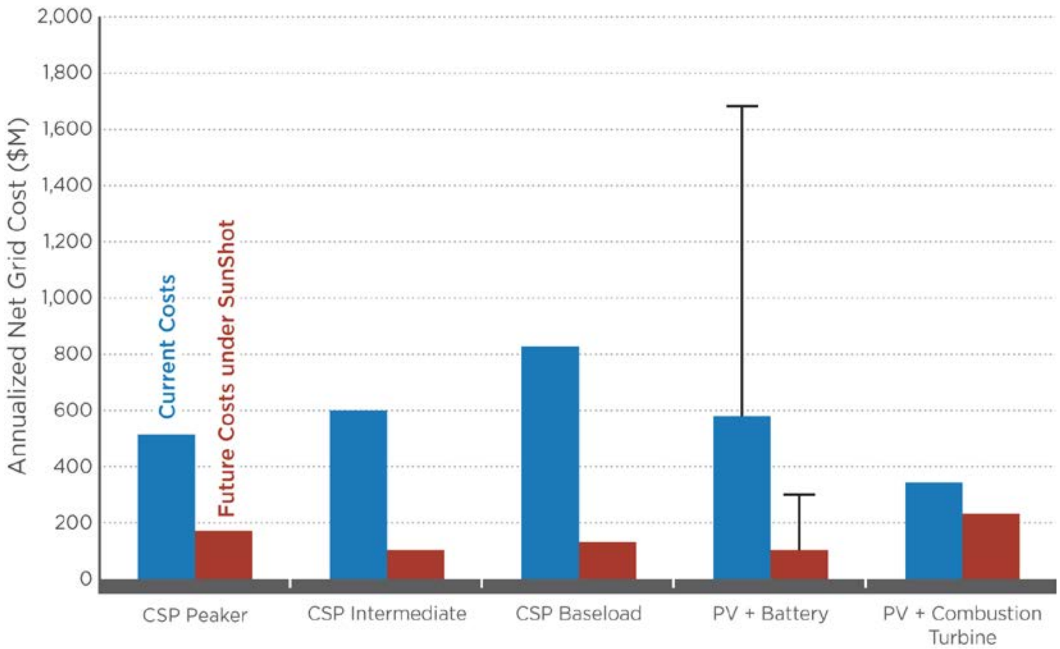


**Figure 20. Annualized net cost results for analysis of current and future cost scenarios for CSP, PV with batteries, and PV with combustion turbines**

CSP peaker, intermediate load, and baseload configurations are identical to those shown in Figure 18.

Figure 20 indicates that under current technology costs, the least-expensive option considered is a combination of solar PV and gas CTs. This result is not surprising because CSP-TES and grid-scale batteries are relatively immature technologies. Current costs also indicate that the lowest-cost CSP configuration (a peaker with a smaller relative solar field) has a lower net cost than the entire range of battery costs considered. Due to currently high heliostat costs, higher-capacity-factor plants with larger solar fields (i.e., intermediate and baseload CSP plants) have a higher net first-year cost despite higher energy output.

These results change when considering future costs. First, both CSP and the lower range of PV-plus-battery costs give a lower net cost than PV with gas CTs, echoing the results from Section 5.2. The most optimal configuration of CSP (now an intermediate-load plant) is lower cost than the range of PV-plus-battery costs considered. Note that the optimal configuration of a CSP plant shifted toward a plant with a higher capacity factor, due to the reduced cost of the solar field under SunShot targets.

# 6 Conclusions

Since the *SunShot Vision Study* (DOE 2012) was published, the non-incentivized LCOE for CSP has fallen significantly from 20.6 cents/kWh for an oil-based parabolic trough with no thermal energy storage—which represented the latest commercial CSP plant constructed in the U.S. at that time—to a projected LCOE of 12.0 cents/kWh based on NREL's estimate for the cost and performance of a current-generation molten-salt power tower with 10 hours of storage.

The primary reason for this almost 30% drop in LCOE has been the introduction of commercially deployed molten-salt power-tower technology in the U.S. and abroad. For the U.S., in particular, the successful deployment of more than 1,200 MW of new capacity—including the first molten-salt tower plant—has been driven by three factors. The first was the Federal Loan Guarantee program, which provided access to federally guaranteed low-cost debt. The second was a 30% investment tax credit made available for solar technologies deployed prior to the end of 2016 and now extended through 2019. The third was the need for states in the Southwest to meet their regional renewable portfolio standards.

Cost reductions are certainly encouraging. But the availability of low-cost PV systems presents a formidable challenge to the continued growth of CSP in the United States and throughout the world. To successfully meet this challenge, developers of CSP systems must continue to address the technology barriers and cost and performance improvement opportunities identified in the *SunShot Vision Study* (DOE 2012). Although substantial progress has lowered the cost and increased the performance of solar fields for both parabolic trough and tower systems, today's systems still rely on being integrated with conventional Rankine-cycle power blocks that operate at a maximum temperature of about 540 °C. To meet SunShot's target of 55% gross power-cycle efficiency, CSP systems must still realize advanced receiver technologies that use high-temperature heat-transfer fluids or particles and minimize thermal losses. Additionally, of critical importance is the development and demonstration of advanced, high-temperature cycles such as supercritical $CO_2$ or air-Brayton cycles integrated with CSP solar fields.

Reducing the cost of CSP systems is vital to successful deployment in future, non-subsidized markets. However, the value of the dispatchability offered by CSP integrated with TES plays an important role in differentiating CSP from variable-generation renewable technologies such as PV and wind. This value will become increasingly apparent as PV and wind gain a greater penetration into the regional power markets. From the perspective of grid operators and load-serving entities, CSP offers the critical ability to provide reliable energy and capacity as the net system load shifts to early-morning or late-evening hours—hours when PV does not generate electricity. Prior analysis performed by NREL has quantified this value of CSP; compared to variable-generation PV, CSP with storage has an increased value of up to 6 cents/kWh at high regional penetrations of renewable technologies. Furthermore, this value was realized for systems with low capacity factors—representative of peaking configurations—not investigated in the *SunShot Vision Study* (DOE 2012).

The increased value demonstrated by CSP for non-baseload configurations highlights the need for an alternative metric when comparing CSP with non-dispatchable options. An analysis of the net system cost provides such an alternative that accounts for the cost of the technology as well as the energy and reliability benefits provided to the regional grid. An assessment of the net system cost indicates that successfully achieving the SunShot component-level cost and performance targets will result in CSP being an attractive alternative to conventional combustion turbine or combined-cycle plants, even at today's low prices for natural gas. This is particularly true for CSP configurations having low and medium capacity factors. CSP is also an attractive option when compared to PV with batteries, especially when considering the uncertainty of current and future battery costs and lifetimes.

# References

Barbose, G., J. Miller, B. Sigrin, E. Reiter, K. Cory, J. McLaren, J. Seel, A. Mills, N. Darghouth, and A. Satchwell. 2016. *On the Path to SunShot: Utility Regulatory and Business Model Reforms for Addressing the Financial Impacts of Distributed Solar on Utilities*. Golden, CO: National Renewable Energy Laboratory. NREL/TP-6A20-65670. http://www.nrel.gov/docs/fy16osti/65670.pdf.

Bayar, T., "Alstom to build 121 MW concentrating solar plant in Israel," *Power Engineering International*, Posted August 7, 2014.

Bolinger, M. and J. Seel, Utility-Scale Solar 2014: An Empirical Analysis of Project Cost, Performance, and Pricing Trends in the United States, Lawrence Berkeley National Laboratory, LBNL-1000917 (Sept. 2015).

Brinkman, G., Renewable Electricity Futures: Operational Analysis of the Western Interconnection at Very High Renewable Penetrations, 53 pp.; NREL Report No. TP-6A20-64467 (2015)

Chung, D., K. Horowitz, and P. Kurup. 2016. *On the Path to SunShot: Emerging Opportunities and Challenges in U.S. Solar Manufacturing*. Golden, CO: National Renewable Energy Laboratory. NREL/TP-7A40-65788. http://www.nrel.gov/docs/fy16osti/65788.pdf.

CPUC, 2015 Filing Guide for System, Local and Flexible Resource Adequacy (RA) Compliance Filings Issued: September 9, 2014 (2014).

Denholm, P. and M. Hummon, Simulating the Value of Concentrating Solar Power with Thermal Energy Storage in a Production Cost Model, NREL Report No. NREL/TP-6A20-56731 (2012)

Denholm, P., K. Clark, and M. O'Connell. 2016. *On the Path to SunShot: Emerging Issues and Challenges in Integrating High Levels of Solar into the Electrical Generation and Transmission System*. Golden, CO: National Renewable Energy Laboratory. NREL/TP-6A20-65800. http://www.nrel.gov/docs/fy16osti/65800.pdf.

Denholm, P., Y.-H. Wan, M. Hummon, and M. Mehos, An Analysis of Concentrating Solar Power with Thermal Energy Storage in a California 33% Renewable Scenario, 26 pp.; NREL Report No. TP-6A20-58186 (2013).

DOE (U.S. Department of Energy). 2012. "SunShot Vision Study." Washington, DC: U.S. Department of Energy. DOE/GO-102012-3037. http://www.nrel.gov/docs/fy12osti/47927.pdf.

EPRI. Solar Thermocline Storage Systems: Preliminary Design Study. Electric Power Research Institute, Palo Alto, CA: June 2010 (2010).

Feldman, D., and M. Bolinger. 2016. *On the Path to SunShot: Emerging Opportunities and Challenges in Financing Solar*. Golden, CO: National Renewable Energy Laboratory. NREL/TP-6A20-65638. http://www.nrel.gov/docs/fy16osti/65638.pdf.

HELI-SCSP, “Abengoa secures for its Concentrated Solar Power (CSP) and Photovoltaic (PV) plants in Chile,” *Solar Thermal Energy News*, Posted: Dec. 31, 2014.

HELI-SCSP, “SolarReserve wants to install 80 MW of solar energy in Chile, Photovoltaic and Concentrated Solar Power (CSP),” *Solar Thermal Energy News*, Posted: Jan. 22, 2015.

HELI-SCSP, “Concentrated solar power (CSP) opportunity in China’s new market,” *Solar Thermal Energy News*, Posted: Nov. 18, 2015.

Hill, J.S., Price of US distributed solar fell 10-20% in 2014, trend continuing in 2015,” *CleanTechnica*, Posted: Aug. 13, 2015.

Ho, C.K., 2015, Review of Avian Mortality Studies at Concentrating Solar Power Plants, in SolarPACES 2015, Cape Town, South Africa, October 13 - 16, 2015.

Ho, C.K., C.A. Sims, and J.M. Christian, 2015, Evaluation of Glare at the Ivanpah Solar Electric Generating System, International Conference on Concentrating Solar Power and Chemical Energy Systems, SolarPACES 2014, 69, 1296-1305 (2015).

Hoeven, M., Technology Roadmap – Solar Thermal Electricity, International Energy Agency, 2014 Ed. (2014).

H.T. Harvey and Associates, Ivanpah Solar Electric Generating System Avian and Bat Monitoring Plan—2013–2014 Annual Report (Revised), H.T Harvey & Associates, Ecological Consultants, Fresno, CA (April 2015).

IEA Technology Roadmap: Solar Thermal Electricity, OECD/IEA, Paris (2014).

IRENA Report, Concentrating Solar Power, Technology Brief E10, IEA-ETSAP, 2013.

Jorgenson, J., P. Denholm, and M. Mehos, Estimating the Value of Utility-Scale Solar Technologies in California Under a 40% Renewable Portfolio Standard. 32 pp.; NREL Report No. TP-6A20-61685 (2014).

Jorgenson, J., M. Mehos, and P. Denholm, Comparing the Net Cost of CSP-TES to PV Deployed with Battery Storage, 2015 SolarPACES Symposium, Cape Town, South Africa (2015).

Kutscher, C., M. Mehos, C. Turchi, G. Glatzmaier, and T. Moss, Line-Focus Solar Power Plant Cost Reduction Plan (Milestone Report). 45 pp.; NREL Report No. TP-5500-48175 (2010).

Kolb, G.J., Evaluation of Annual Performance of 2-Tank and Thermocline Thermal Storage for Trough Plants, SolarPACES 2010, Perpignan, France (2010).

Kolb, G.J., C.K. Ho, T.R. Mancini, and J.A. Gary, Power Tower Technology Roadmap and Cost Reduction Plan. 38 pp.; Sandia Report SAND2011-2419 (2011).

Kurup, P. and C. Turchi, Parabolic Trough Collector Cost Update for the System Advisor Model (SAM), National Renewable Energy Laboratory, Technical Report NREL/TP-6A20-65228 (Nov. 2015).

Madaeni, S.H., R. Sioshansi, and P. Denholm, Capacity Value of Concentrating Solar Power Plants, 40 pp.; NREL Report No. TP-6A20-51253 (2011).

McCrary, M.D., R.L. McKernan, R.W. Schreiber, W.D. Wagner, and T.C. Sciarrotta, Avian Mortality at a Solar-Energy Power-Plant, *Journal of Field Ornithology*, 57(2), 135–141 (1986).

Mehos, M., C. Turchi, J. Jorgenson, P. Denholm, C. Ho, and K. Armijo.2016. *On the Path to SunShot: Advancing Concentrating Solar Power Technology, Performance, and Dispatchability*. Golden, CO: National Renewable Energy Laboratory. NREL/TP-5500-65668. http://www.nrel.gov/docs/fy16osti/65668.pdf.

Miller, N.W., M. Shao, S. Pajic, and R. D'Aquila, Western Wind and Solar Integration Study Phase 3—Frequency Response and Transient Stability. Technical Report NREL/SR-5D00-62906 (Dec. 2014).

Mills, A. and R. Wiser, An Evaluation of Solar Valuation Methods Used in Utility Planning and Procurement Processes, 87 pp.; LBNL Report 5933E (2012).

Palmintier, B., R. Broderick, B. Mather, M. Coddington, K. Baker, F. Ding, M. Reno, M. Lave, and A. Bharatkumar. 2016. *On the Path to SunShot: Emerging Issues and Challenges in Integrating Solar with the Distribution System*. Golden, CO: National Renewable Energy Laboratory. NREL/TP-5D00-65331. http://www.nrel.gov/docs/fy16osti/65331.pdf.

RED electrica de España (REE), The Spanish Electricity System – Preliminary Report 2013, RED Electrica de Espana, Madrid, Spain, (2014). http://www.ree.es/sites/default/files/downloadable/preliminary_report_2013.pdf

Richardson, J., 50% Renewable Electricity Passed By California Senate, *CleanTechnica*, Posted: June 19, 2015.

Roth, S., "Rice large-scale solar project near Blythe all but dead," The Desert Sun, Posted: Oct. 3, 2014.

Solar Energy Industries Association (SEIA), "SEIA Celebrates Extension of the ITC," SEIA Press Release, Posted: Dec 18, 2015.

Sioshansi, R., S. Madaeni, and P. Denholm, A Dynamic Programming Approach to Estimate the Capacity Value of Energy Storage, *IEEE Transactions on Power Systems* 29, 395–403 (2014).

Stekli, J., DOE CSP Program Manager, personal communications (Dec. 2015).

Tuohy, A. and M. O'Malley, Pumped Storage in Systems with Very High Wind Penetration, *Energy Policy* 39, 1965–1974 (2011).

Turchi, C. and G. Heath, Molten Salt Power Tower Cost Model for the System Advisor Model (SAM), National Renewable Energy Laboratory, Technical Report NREL/TP-5500-57625 (Feb. 2013).

Walston Jr., L.J., K.E Rollins, K.P. Smith, K.E. LaGory, K. Sinclair, C. Turchi, T. Wendelin, and H. Souder, A Review of Avian Monitoring and Mitigation Information at Existing Utility-Scale Solar Facilities, Argonne National Laboratory and the National Renewable Energy Laboratory, Environmental Science Division ANL/EVS-15/2 (April 2015).

Wiser, R., T. Mai, D. Millstein, J. Macknick, A. Carpenter, S. Cohen, W. Cole, B. Frew, and G. A. Heath. 2016. *On the Path to SunShot: The Environmental and Public Health Benefits of Achieving High Penetrations of Solar Energy in the United States*. Golden, CO: National Renewable Energy Laboratory. NREL/TP-6A20-65628. http://www.nrel.gov/docs/fy16osti/65628.pdf.

Woodhouse, M., R. Jones-Albertus, D. Feldman, R. Fu, K. Horowitz, D. Chung, D. Jordan, and S. Kurtz. 2016. *On the Path to SunShot: The Role of Advancements in Solar Photovoltaic Efficiency, Reliability, and Costs*. Golden, CO: National Renewable Energy Laboratory. NREL/TP-6A20-65464. http://www.nrel.gov/docs/fy16osti/65464.pdf.

Woods, L., "Green light for Abengoa CSP plant in Chile," PVTech, Posted May 12, 2014.